

# ERROR ESTIMATES FOR A VORTICITY-BASED VELOCITY-STRESS FORMULATION OF THE STOKES EIGENVALUE PROBLEM\*

FELIPE LEPE<sup>†</sup>, GONZALO RIVERA<sup>‡</sup>, AND JESUS VELLOJIN<sup>§</sup>

**Abstract.** The aim of this paper is to analyze a mixed formulation for the two dimensional Stokes eigenvalue problem where the unknowns are the stress and the velocity, whereas the pressure can be recovered with a simple postprocess of the stress. The stress tensor is written in terms of the vorticity of the fluid, leading to an alternative mixed formulation that incorporates this physical feature. We propose a mixed numerical method where the stress is approximated with suitable Nédelec finite elements, whereas the velocity is approximated with piecewise polynomials of degree  $k \geq 0$ . With the aid of the compact operators theory we derive convergence of the method and spectral correctness. Moreover, we propose a reliable and efficient a posteriori error estimator for our spectral problem. We report numerical tests in different domains, computing the spectrum and convergence orders, together with a computational analysis for the proposed estimator. In addition, we use the corresponding error estimator to drive an adaptive scheme, and we report the results of a numerical test, that allow us to assess the performance of this approach.

**Key words.** Stokes equations, eigenvalue problems, error estimates, a posteriori error estimates, mixed problems

**AMS subject classifications.** 35Q35, 65N15, 65N25, 65N30, 65N50, 76D07

**1. Introduction.** The Stokes problem is a system of equations that describes the motion of a certain fluid. For an open domain  $\Omega \subset \mathbb{R}^2$  with Lipschitz boundary  $\partial\Omega$ , we are interested in the Stokes eigenvalue problem

$$(1.1) \quad \begin{cases} -\mu\Delta\mathbf{u} + \nabla p = \lambda\mathbf{u} & \text{in } \Omega, \\ \operatorname{div}\mathbf{u} = 0 & \text{in } \Omega, \\ \mathbf{u} = \mathbf{0} & \text{on } \partial\Omega, \end{cases}$$

where  $\mu > 0$  is the kinematic viscosity,  $\mathbf{u}$  is the velocity and  $p$  is the pressure.

In the nowadays there are a number of papers where different formulations, together with numerical methods, have been proposed in order to solve (1.1) [5, 21, 22, 26, 28, 27, 32, 33]. Each of these contributions are concerned in the analysis of mathematical formulations and the development of robust numerical methods that, with high accuracy, are capable to approximate the spectrum of (1.1), namely the eigenvalues and its associated eigenfunctions. Not only the computation of the spectrum has been a subject of study, but also adaptivity strategies when the eigenvalues are not smooth enough and hence, convergence orders of approximation are affected by this lack of regularity.

The development of numerical methods to solve eigenvalue problems, particularly (1.1), is a current subject of study in the community of numerical analysis, since the knowledge of the physical eigenmodes of the spectral Stokes system are important in

---

\*Submitted to the editors DATE.

**Funding:** The first author was partially supported by DIUBB through project 2120173 GI/C Universidad del Bío-Bío and ANID-Chile through FONDECYT project 11200529 (Chile).

<sup>†</sup>GIMNAP-Departamento de Matemática, Universidad del Bío - Bío, Casilla 5-C, Concepción, Chile. [flepe@ubiobio.cl](mailto:flepe@ubiobio.cl).

<sup>‡</sup>Departamento de Ciencias Exactas, Universidad de Los Lagos, Casilla 933, Osorno, Chile. [gonzalo.rivera@ulagos.cl](mailto:gonzalo.rivera@ulagos.cl).

<sup>§</sup>GIMNAP-Departamento de Matemática, Universidad del Bío - Bío, Casilla 5-C, Concepción, Chile.. [jesus.vellojinm@usm.cl](mailto:jesus.vellojinm@usm.cl).

certain applications for the development and design of pipes, structures, containers, dams, etc.. Moreover, not only the velocity and pressure are quantities of interest, but also others as the stress, vorticity, stream functions, just to mention some of the most relevant. It is this need that motivates the analysis of mixed formulations and, hence, mixed numerical methods. These mixed methods have been plenty analyzed for load problems [2, 4, 8, 9, 18, 20] where finite elements, virtual elements, discontinuous methods, just to mention a few, have been considered. These methods and formulations can be explored in order to solve the Stokes spectral problem with an important accuracy.

On the other hand, adaptive mesh refinement strategies based on a posteriori error indicators play a relevant role in the numerical solution of partial differential equations in a general sense. Several approaches have been considered to design error estimators based on the residual equations (see [1, 40] and the references therein). In particular, for the load problem associated to the Stokes equations, we can mention as recent developments [7, 30, 37], whereas for the Stokes spectral problems we refer to [5, 23, 29, 39], and the references therein.

Now, following with our research program related to mixed formulations and their discretizations for eigenvalue problems, the present work introduces a formulation that is inspired in [18] for the load problem, where an augmented method is introduced in order to approximate the velocity, pressure and stress. Despite the fact that this formulation is more expensive since the pressure is directly computed with the method instead of eliminate it, the augmented method is flexible on the choice of families of finite elements. In our case, since we are interested in the spectral problem associated to the Stokes problem, a more simple formulation is enough for this purpose, since the computational costs are reduced, and hence, the computational solvers for eigenvalue problems compute the solutions in less time without loss of accuracy. More precisely, since the solution operator is defined for the velocity component only (cf. Section 2), our primary goal is to compute this unknown (and its associated eigenvalues) and then derive the others quantities of interest in postprocessing. In fact, the pressure and vorticity can be computed using a linear combination of stress and velocity. This is a clear advantage compared with the recent work [28], where the pressure is incorporated in the formulation and the proposed numerical methods, implying more expensive mixed methods. However, the analysis presented in the present study can be perfectly adapted to include the pressure in the preprocessing, with a consequent increase in computational cost.

The contents of our papers are presented as follows: in Section 2 we present the Stokes eigenvalue problem, introducing the stress which we write in terms of the vorticity, leading to a variational formulation where the unknowns are the aforementioned stress and the velocity field. We introduce the solution operator and recall some regularity properties for the eigenfunctions. In Section 3 we introduce the mixed finite elements in which our method is based. Here, we present the finite element spaces, approximation properties and hence, the discrete eigenvalue problem. The discrete solution operator is also defined. In Section 4 we develop the convergence analysis with the compact operators approach. Error estimates for the eigenvalues and eigenfunction are derived. Section 5 is dedicated to an a posteriori error analysis, where we present a residual based a posteriori error analysis, together with the corresponding reliability and efficiency for the proposed estimator. Finally, in Section 6 we report a series of numerical tests to illustrate all our theoretical results. We start with a priori results on different geometries, testing the robustness of our scheme in different orders of approximation. This is followed by an adaptivity test, where we use a non-convex

geometry to verify the performance of the proposed estimator.

**1.1. Preliminaries and notations.** Given any Hilbert space  $X$ , let  $X^2$  and  $\mathbb{X}$  denote, respectively, the space of vectors and tensors with entries in  $X$ . In particular,  $\mathbb{I}$  is the identity matrix of  $\mathbb{R}^{2 \times 2}$ , and  $\mathbf{0}$  denotes a generic null vector or tensor. Given  $\boldsymbol{\tau} := (\tau_{ij})$  and  $\boldsymbol{\sigma} := (\sigma_{ij}) \in \mathbb{R}^{2 \times 2}$ , we define, as usual, the tensor inner product  $\boldsymbol{\tau} : \boldsymbol{\sigma} := \sum_{i,j=1}^2 \tau_{ij} \sigma_{ij}$ .

Let  $\Omega$  be a polygonal Lipschitz bounded domain of  $\mathbb{R}^2$  with boundary  $\partial\Omega$ . For  $s \geq 0$ ,  $\|\cdot\|_{s,\Omega}$  stands indistinctly for the norm of the Hilbertian Sobolev spaces  $H^s(\Omega)$ ,  $H^s(\Omega)^2$  or  $\mathbb{H}^s(\Omega) := H^s(\Omega)^{2 \times 2}$  for scalar, vectorial and tensorial fields, respectively, with the convention  $H^0(\Omega) := L^2(\Omega)$ ,  $H^0(\Omega)^2 = L^2(\Omega)^2$  and  $\mathbb{H}^0(\Omega) := \mathbb{L}^2(\Omega)$ . We also define for  $s \geq 0$  the Hilbert space  $\mathbb{H}(\mathbf{curl}; \Omega) := \{\boldsymbol{\tau} \in \mathbb{L}^2(\Omega) : \mathbf{curl}(\boldsymbol{\tau}) \in L(\Omega)^2\}$ , whose norm is given by  $\|\boldsymbol{\tau}\|_{\mathbf{curl},\Omega}^2 := \|\boldsymbol{\tau}\|_{0,\Omega}^2 + \|\mathbf{curl}(\boldsymbol{\tau})\|_{0,\Omega}^2$ . The relation  $\mathbf{a} \lesssim \mathbf{b}$  indicates that  $\mathbf{a} \leq C\mathbf{b}$ , with a positive constant  $C$  which is independent of  $\mathbf{a}$ ,  $\mathbf{b}$  and the mesh size  $h$ , which will be introduced in Section 3.

Let us define the tensors

$$\mathbb{J} := \begin{pmatrix} 0 & 1 \\ -1 & 0 \end{pmatrix} \quad \text{and} \quad \boldsymbol{\tau}^r := \boldsymbol{\tau} - \frac{1}{2}(\boldsymbol{\tau} : \mathbb{J})\mathbb{J} \quad \forall \boldsymbol{\tau} \in \mathbb{R}^{2 \times 2},$$

where the relation  $\boldsymbol{\tau}^r : \mathbb{J} = 0$  holds.

Let  $\boldsymbol{\varphi} = (\varphi_1, \varphi_2)^\dagger$  and  $\boldsymbol{\tau} = (\tau_{ij})$  be vector- and tensor-valued fields, respectively, we define

$$\mathbf{curl}(\boldsymbol{\varphi}) := \begin{pmatrix} -\frac{\partial \varphi_1}{\partial x_2} & \frac{\partial \varphi_1}{\partial x_1} \\ -\frac{\partial \varphi_2}{\partial x_2} & \frac{\partial \varphi_2}{\partial x_1} \end{pmatrix}, \quad \text{and} \quad \mathbf{curl}(\boldsymbol{\tau}) := \begin{pmatrix} \frac{\partial \tau_{12}}{\partial x_1} - \frac{\partial \tau_{11}}{\partial x_2} \\ \frac{\partial \tau_{22}}{\partial x_1} - \frac{\partial \tau_{21}}{\partial x_2} \end{pmatrix}.$$

Finally, through our paper, we denote by  $\text{div}$  and  $\mathbf{div}$  the divergence operator when is applied to vectorial and tensorial fields, respectively.

**2. The model problem.** Let  $\Omega \subset \mathbb{R}^2$  be an open bounded domain with Lipschitz boundary  $\partial\Omega$ . Let us write the stress tensor  $\boldsymbol{\sigma}$  in terms of the vorticity as follows  $\boldsymbol{\sigma} := \mu \mathbf{curl}(\mathbf{u}) - p\mathbb{J}$ . From this relation, we observe that the vorticity of the fluid can be recovered with the relation  $\mathbf{curl}(\mathbf{u}) = \frac{1}{\mu}(\boldsymbol{\sigma} + p\mathbb{J})$ .

Since  $\Delta \mathbf{u} = \mathbf{curl}(\mathbf{curl}(\mathbf{u}))$  and  $\mathbf{curl}(p\mathbb{J}) = \nabla p$ , the first equation on system (1.1) is rewritten as  $\mathbf{curl}(\boldsymbol{\sigma}) = -\lambda \mathbf{u}$  in  $\Omega$ .

On the other hand, the identity  $\text{div}(\mathbf{u}) = \mathbf{curl}(\mathbf{u}) : \mathbb{J}$  holds, and hence, the second equation on (1.1) is rewritten as  $\mathbf{curl}(\mathbf{u}) : \mathbb{J} = 0$  in  $\Omega$ . With these relations at hand, (1.1) now reads as follows: Find the stress  $\boldsymbol{\sigma}$ , the velocity  $\mathbf{u}$  and the pressure  $p$  such that

$$(2.1) \quad \begin{cases} \boldsymbol{\sigma} - \mu \mathbf{curl}(\mathbf{u}) + p\mathbb{J} = \mathbf{0} & \text{in } \Omega, \\ \mathbf{curl}(\boldsymbol{\sigma}) = -\lambda \mathbf{u} & \text{in } \Omega, \\ \mathbf{curl}(\mathbf{u}) : \mathbb{J} = 0 & \text{in } \Omega, \\ \mathbf{u} = \mathbf{0} & \text{on } \partial\Omega. \end{cases}$$

Algebraic manipulations reveal that the pressure satisfies  $p = -1/2(\boldsymbol{\sigma} : \mathbb{J})$ . Hence, we can eliminate the pressure on (2.1) leading to the following equivalent system

$$(2.2) \quad \begin{cases} \boldsymbol{\sigma}^r - \mu \mathbf{curl}(\mathbf{u}) = \mathbf{0} & \text{in } \Omega, \\ \mathbf{curl}(\boldsymbol{\sigma}) = -\lambda \mathbf{u} & \text{in } \Omega, \\ \mathbf{u} = \mathbf{0} & \text{on } \partial\Omega. \end{cases}$$

Now, a variational formulation for (2.2) reads as follows: Find  $\lambda \in \mathbb{R}$  and  $\mathbf{0} \neq (\boldsymbol{\sigma}, \mathbf{u}) \in \mathbb{H}(\mathbf{curl}, \Omega) \times L^2(\Omega)^2$  such that

$$(2.3) \quad a(\boldsymbol{\sigma}, \boldsymbol{\tau}) + b(\boldsymbol{\tau}, \mathbf{u}) = 0 \quad \forall \boldsymbol{\tau} \in \mathbb{H}(\mathbf{curl}, \Omega),$$

$$(2.4) \quad b(\boldsymbol{\sigma}, \mathbf{v}) = -\lambda(\mathbf{u}, \mathbf{v})_{0,\Omega} \quad \forall \mathbf{v} \in L^2(\Omega)^2.$$

Let us define the spaces  $\mathbb{H} := \mathbb{H}(\mathbf{curl}, \Omega)$  and  $\mathbf{Q} := L^2(\Omega)^2$ . With these definitions at hand, we introduce the bilinear forms  $a : \mathbb{H} \times \mathbb{H} \rightarrow \mathbb{R}$  and  $b : \mathbb{H} \times \mathbf{Q} \rightarrow \mathbb{R}$  defined as follows

$$a(\boldsymbol{\xi}, \boldsymbol{\tau}) := \frac{1}{\mu} \int_{\Omega} \boldsymbol{\xi}^r : \boldsymbol{\tau}^r \quad \text{and} \quad b(\boldsymbol{\xi}, \mathbf{v}) := \int_{\Omega} \mathbf{v} \cdot \mathbf{curl}(\boldsymbol{\xi}) \quad \forall \boldsymbol{\xi}, \boldsymbol{\tau} \in \mathbb{H}, \forall \mathbf{v} \in \mathbf{Q}.$$

For our analysis, let us consider the decomposition

$$(2.5) \quad \mathbb{H}(\mathbf{curl}, \Omega) = \mathbb{H}_0 \oplus \mathbb{R}\mathbb{J},$$

where

$$\mathbb{H}_0 := \left\{ \boldsymbol{\tau} \in \mathbb{H} : \int_{\Omega} \boldsymbol{\tau} : \mathbb{J} = 0 \right\}.$$

The need of this space is motivated due the non-uniqueness of solution of (2.3)–(2.4). To make matter precise, for any  $c \in \mathbb{R}$ , the duo  $(c\mathbb{J}, \mathbf{0})$  is a solution of the homogeneous problem associated to (2.3)–(2.4). Now, we write the following eigenvalue problem: find  $\lambda \in \mathbb{R}$  and  $\mathbf{0} \neq (\boldsymbol{\sigma}, \mathbf{u}) \in \mathbb{H}_0 \times \mathbf{Q}$  such that

$$(2.6) \quad a(\boldsymbol{\sigma}, \boldsymbol{\tau}) + b(\boldsymbol{\tau}, \mathbf{u}) = 0 \quad \forall \boldsymbol{\tau} \in \mathbb{H}_0,$$

$$(2.7) \quad b(\boldsymbol{\sigma}, \mathbf{v}) = -\lambda(\mathbf{u}, \mathbf{v})_{0,\Omega} \quad \forall \mathbf{v} \in \mathbf{Q}.$$

We recall some important results that allows us to establish the well posedness of our mixed formulation. The following result is instrumental.

LEMMA 2.1. *There exists a constant  $C > 0$ , depending on  $\Omega$ , such that for all  $\boldsymbol{\tau} \in \mathbb{H}_0$  there holds*

$$C\|\boldsymbol{\tau}\|_{0,\Omega}^2 \leq \|\boldsymbol{\tau}^r\|_{0,\Omega}^2 + \|\mathbf{curl}(\boldsymbol{\tau})\|_{0,\Omega}^2.$$

*Proof.* See [18, Lemma 2.3]. □

Let us introduce the the kernel of  $b(\cdot, \cdot)$ , defined as the following space

$$\mathbb{V} := \{\boldsymbol{\tau} \in \mathbb{H}_0 : b(\boldsymbol{\tau}, \mathbf{v}) = 0 \forall \mathbf{v} \in L^2(\Omega)^2\} = \{\boldsymbol{\tau} \in \mathbb{H}_0 : \mathbf{curl}(\boldsymbol{\tau}) = \mathbf{0} \text{ in } \Omega\},$$

in which, according to Lemma 2.1,  $a(\cdot, \cdot)$  is coercive (see [18, Theorem 2.4]). Also, the bilinear form  $b(\cdot, \cdot)$  satisfies the following inf-sup condition (see [18, Theorem 2.2])

$$(2.8) \quad \sup_{\mathbf{0} \neq \boldsymbol{\tau} \in \mathbb{H}_0} \frac{\int_{\Omega} \mathbf{v} \cdot \mathbf{curl}(\boldsymbol{\tau})}{\|\boldsymbol{\tau}\|_{\mathbf{curl}, \Omega}} \geq \beta \|\mathbf{v}\|_{0,\Omega} \quad \forall \mathbf{v} \in \mathbf{Q},$$

where  $\beta$  is a positive constant.

With these ingredients at hand, we are in position to introduce the solution operator

$$\mathbf{T} : \mathbf{Q} \rightarrow \mathbf{Q}, \quad \mathbf{f} \mapsto \mathbf{T}\mathbf{f} := \hat{\mathbf{u}},$$



where the pair  $(\hat{\boldsymbol{\sigma}}, \hat{\mathbf{u}}) \in \mathbb{H}_0 \times \mathbf{Q}$  is the solution of the following well posed source problem

$$(2.9) \quad a(\hat{\boldsymbol{\sigma}}, \boldsymbol{\tau}) + b(\boldsymbol{\tau}, \hat{\mathbf{u}}) = 0 \quad \forall \boldsymbol{\tau} \in \mathbb{H}_0,$$

$$(2.10) \quad b(\hat{\boldsymbol{\sigma}}, \mathbf{v}) = -(\mathbf{f}, \mathbf{v})_{0,\Omega} \quad \forall \mathbf{v} \in \mathbf{Q},$$

implying that  $\mathbf{T}$  is well defined due to the Babuška-Brezzi theory. Moreover, we have the following estimate

$$\|\hat{\boldsymbol{\sigma}}\|_{\mathbf{curl},\Omega} + \|\hat{\mathbf{u}}\|_{0,\Omega} \lesssim \|\mathbf{f}\|_{0,\Omega}.$$

Therefore, recalling that the continuous dependence result given above is equivalent to the global inf-sup condition for the continuous formulation (2.9)–(2.10). i.e:

$$(2.11) \quad \|(\boldsymbol{\tau}, \mathbf{v})\|_{\mathbb{H}_0 \times \mathbf{Q}} \lesssim \sup_{\substack{(\boldsymbol{\xi}, \mathbf{w}) \in \mathbb{H}_0 \times \mathbf{Q} \\ (\boldsymbol{\xi}, \mathbf{w}) \neq 0}} \frac{a(\boldsymbol{\tau}, \boldsymbol{\xi}) + b(\boldsymbol{\xi}, \mathbf{v}) + b(\boldsymbol{\tau}, \mathbf{w})}{\|(\boldsymbol{\xi}, \mathbf{w})\|_{\mathbb{H}_0 \times \mathbf{Q}}}.$$

Elementary computations reveal that  $\mathbf{T}$  is selfadjoint respect to the  $L^2$  inner product. We also observe that the triplet  $(\lambda, (\boldsymbol{\sigma}, \mathbf{u})) \in \mathbb{R} \times \mathbb{H}_0 \times \mathbf{Q}$  solves (2.6)–(2.7) if and only if  $(\kappa, \mathbf{u})$  is an eigenpair of  $\mathbf{T}$ , i.e.  $\mathbf{T}\mathbf{u} = \kappa\mathbf{u}$  with  $\kappa := 1/\lambda$ .

From [17, 38] we have the following regularity result for the Stokes spectral problem.

**THEOREM 2.2.** *If  $(\mathbf{u}, p, \lambda) \in H_0^1(\Omega)^2 \times L_0^2(\Omega) \times \mathbb{R}$  solves (1.1), there exists  $s > 0$  such that  $\mathbf{u} \in H^{1+s}(\Omega)^2$  and  $p \in H^s(\Omega)$ .*

We observe that Theorem 2.2, together with the first and second equations of (2.2) reveal that  $\mathbf{curl}(\boldsymbol{\sigma}) \in H^{1+s}(\Omega)^2$  and  $\boldsymbol{\sigma} \in \mathbb{H}^s(\Omega)$ , respectively. This additional regularity for the stress tensor is a key ingredient for the numerical approximation.

*Remark 2.3.* Note that the estimate

$$\|\hat{\boldsymbol{\sigma}}\|_{s,\Omega} + \|\hat{\mathbf{u}}\|_{1+s,\Omega} \lesssim \|\mathbf{f}\|_{0,\Omega}$$

holds. This allows us to conclude that  $\mathbf{T}$  is compact, where its spectrum satisfies  $\text{sp}(\mathbf{T}) = \{0\} \cup \{\mu_k\}_{k \in \mathbb{N}}$ , where  $\{\mu_k\}_{k \in \mathbb{N}} \in (0, 1)$  is a sequence of real positive eigenvalues which converges to zero, repeated according their respective multiplicities.

**3. The mixed finite element method.** In this section we introduce and analyze the mixed finite element method to approximate the eigenvalues and eigenfunctions of (2.6)–(2.7). With this goal in mind, we begin by introducing a regular family of triangulations of  $\Omega$  denoted by  $\{\mathcal{T}_h\}_{h>0}$ . Let  $h_T$  the diameter of a triangle  $T$  of the triangulation and let us define  $h := \max\{h_T : T \in \mathcal{T}_h\}$ .

**3.1. The finite element spaces.** Let us introduce suitable spaces to approximate the stress, the velocity and pressure. For  $v \geq 0$  and  $B \subset \mathbb{R}^2$  being a subset of the plane we denote by  $P_v(B)$  the space of polynomials of degree at most  $v$  defined on  $B$  and by  $\tilde{P}_v(B)$  the subspace of homogeneous polynomials of degree  $v$ .

We consider the local Nédelec space of the first type and order  $k \geq 0$ ,

$$\text{NED}_k^{(1)}(T) := P_k(T)^2 \oplus \tilde{P}_{k+1}(T)^2.$$

Hence, the global Nédelec space of the first type is defined by

$$\text{NED}_k^{(1)}(\mathcal{T}_h) := \left\{ \boldsymbol{\tau} \in \mathbb{H}(\mathbf{curl}, \Omega) : \boldsymbol{\tau}|_T \in \text{NED}_k^{(1)}(T), \forall T \in \mathcal{T}_h \right\},$$

where  $\boldsymbol{\tau}|_T^{\mathfrak{t}}$  must be understood as  $(\tau_{i1}, \tau_{i2})$ , for  $i = 1, 2$ .

Similarly, the local Nédelec space of the second type and order  $k + 1$  is given by

$$\mathbf{NED}_{k+1}^{(2)}(T) := \mathbf{P}_{k+1}(T)^2 \quad \text{with } k \geq 0,$$

whereas the corresponding global space is defined by

$$\mathbf{NED}_{k+1}^{(2)}(\mathcal{T}_h) := \left\{ \boldsymbol{\tau} \in \mathbb{H}(\mathbf{curl}, \Omega) : \boldsymbol{\tau}|_T^{\mathfrak{t}} \in \mathbf{NED}_{k+1}^{(2)}(T), \forall T \in \mathcal{T}_h \right\}.$$

We also consider the the space of piecewise polynomials of degree at most  $k$ ,

$$\mathbf{P}_k(\mathcal{T}_h) := \{q \in L^2(\Omega) : q|_T \in \mathbf{P}_k(T) \forall T \in \mathcal{T}_h\}.$$

*Remark 3.1.* It is well known from the literature that  $\mathbf{RT}_{k-1} \subset \mathbf{BDM}_k \subset \mathbf{RT}_k$  for all  $k \geq 1$  (see [10, Section 2]). This is important to notice since  $\mathbf{NED}_k^{(1)}$  and  $\mathbf{NED}_k^{(2)}$  are just rotated Raviart-Thomas and Brezzi-Douglas-Marini families, respectively. This allows us to conclude that the number of degrees of freedom per edge is the same for both finite elements. However, the number of internal degrees of freedom of  $\mathbf{NED}_k^{(2)}$  elements is less than that of standard finite elements of the same order such as  $\mathbf{NED}_k^{(1)}$ . A count of the internal degrees of freedom for in two dimensions gives

$$\mathbf{NED}_k^{(2)} : 2(k-1)(k+1) \quad \mathbf{NED}_k^{(1)} : 2k(k+1).$$

**3.2. Approximation errors.** In the following, some approximation results for discrete spaces are presented. To make matters precise, since we consider two spaces to approximate the stress tensor, we need to introduce suitable interpolators for the Nédelec spaces defined above. We begin with the classical approximation property for piecewise polynomials (see [10]). Let  $\mathcal{R}_h : L^2(\Omega)^2 \rightarrow \mathbf{P}_k(\mathcal{T}_h)^2$ . The following estimate holds

$$\|\mathbf{v} - \mathcal{R}_h \mathbf{v}\|_{0,\Omega} \lesssim h^{\min\{t, k+1\}} \|\mathbf{v}\|_{t,\Omega} \quad \forall \mathbf{v} \in \mathbf{H}^t(\Omega)^2 \cap L^2(\Omega)^2.$$

Let  $\boldsymbol{\Pi}_h^{\mathbf{NED}^{(\ell)}} : \mathbb{H}(\Omega)^t \rightarrow \mathbf{NED}_{\ell+k-1}^{(\ell)}$ , with  $t > 1/2$ , be the tensorial Nédelec interpolation operator (see [34, Section 5.5]), where the superindex  $\ell \in \{1, 2\}$  represents any of the Nédelec families that we are considering.

The following commuting diagram property holds

$$(3.1) \quad \mathbf{curl}(\boldsymbol{\Pi}_h^{\mathbf{NED}^{(\ell)}}(\boldsymbol{\tau})) = \mathcal{R}_h(\mathbf{curl}(\boldsymbol{\tau})).$$

Moreover, the following estimate holds (see [35, Theorem 2] and [36, Proposition 3])

$$(3.2) \quad \|\boldsymbol{\tau} - \boldsymbol{\Pi}_h^{\mathbf{NED}^{(\ell)}} \boldsymbol{\tau}\|_{0,\Omega} \lesssim h^{\min\{t, \ell+k\}} \|\boldsymbol{\tau}\|_{t,\Omega} \quad \forall \boldsymbol{\tau} \in \mathbb{H}^t(\Omega), \quad t \geq 1 - (\ell - 1)/2.$$

Also, thanks to (3.1), if  $\mathbf{curl}(\boldsymbol{\tau}) \in \mathbf{H}^t(\Omega)^2$  with  $t \geq 0$  we have the following result

$$(3.3) \quad \|\mathbf{curl}(\boldsymbol{\tau} - \boldsymbol{\Pi}_h^{\mathbf{NED}^{(\ell)}} \boldsymbol{\tau})\|_{0,\Omega} = \|\mathbf{curl}(\boldsymbol{\tau}) - \mathcal{R}_h(\mathbf{curl}(\boldsymbol{\tau}))\|_{0,\Omega} \lesssim h^{\min\{t, k+1\}} \|\mathbf{curl}(\boldsymbol{\tau})\|_{t,\Omega}.$$

Defining  $\boldsymbol{\Pi}_h^{\mathbf{NED}^{(\ell)}}$  as  $\boldsymbol{\Pi}_h^{\mathbf{NED}^{(\ell)}} : \mathbb{H}^t(\Omega) \cap \mathbb{H}(\mathbf{curl}, \Omega) \rightarrow \mathbf{NED}_k^{(\ell)}$  for all  $t \in (0, 1 - (\ell - 1)/2]$ , the following estimate holds (see [34, Theorem 5.41] and [36, Proposition 3])

$$(3.4) \quad \|\boldsymbol{\tau} - \boldsymbol{\Pi}_h^{\mathbf{NED}^{(\ell)}} \boldsymbol{\tau}\|_{0,\Omega} \lesssim h^t (\|\boldsymbol{\tau}\|_{t,\Omega} + \|\mathbf{curl}(\boldsymbol{\tau})\|_{0,\Omega}) \quad \boldsymbol{\tau} \in \mathbb{H}^t(\Omega) \cap \mathbb{H}(\mathbf{curl}, \Omega).$$

For  $\ell \in \{1, 2\}$ , we introduce the following spaces

$$\mathbb{H}_{0,h} := \left\{ \boldsymbol{\tau} \in \mathbf{NED}_{\ell+k-1}^{(\ell)} : \int_{\Omega} \boldsymbol{\tau}_h : \mathbb{J} = 0 \right\}, \quad \mathbf{Q}_h := \mathbf{P}_k(\mathcal{T}_h)^2.$$

**3.3. Discrete eigenvalue problems.** In what follows, we present the finite element discretization of the spectral problem (2.6)–(2.7). With the finite element spaces defined previously, we have the following discrete problem: Find  $\lambda_h$  and  $\mathbf{0} \neq (\boldsymbol{\sigma}_h, \mathbf{u}_h) \in \mathbb{H}_{0,h} \times \mathbf{Q}_h$  such that

$$(3.5) \quad a(\boldsymbol{\sigma}_h, \boldsymbol{\tau}_h) + b(\boldsymbol{\tau}_h, \mathbf{u}_h) = 0 \quad \forall \boldsymbol{\tau}_h \in \mathbb{H}_{0,h},$$

$$(3.6) \quad b(\boldsymbol{\sigma}_h, \mathbf{v}_h) = -\lambda_h (\mathbf{u}_h, \mathbf{v}_h)_{0,\Omega} \quad \forall \mathbf{v}_h \in \mathbf{Q}_h.$$

Now our interest is to analyze the well posedness of (3.5)–(3.6). With this purpose, we begin with the following discrete inf-sup for  $b(\cdot, \cdot)$ , whose proof is inspired by [20, Lemma 3.2].

LEMMA 3.2. *There exists a positive constant  $\widehat{\beta}$ , independent of  $h$ , such that*

$$(3.7) \quad \sup_{\mathbf{0} \neq \boldsymbol{\tau}_h \in \mathbb{H}_{0,h}} \frac{\int_{\Omega} \mathbf{v}_h \cdot \mathbf{curl}(\boldsymbol{\tau}_h)}{\|\boldsymbol{\tau}_h\|_{\mathbf{curl},\Omega}} \geq \widehat{\beta} \|\mathbf{v}\|_{0,\Omega} \quad \forall \mathbf{v}_h \in \mathbf{Q}_h.$$

*Proof.* Since we already have the continuous inf-sup condition (2.8), it will be enough to construct a Fortin operator to guarantee that  $b(\cdot, \cdot)$  satisfies a discrete inf-sup condition. Indeed, let  $\widetilde{\Omega}$  be a convex polygonal domain such that  $\Omega \subseteq \widetilde{\Omega}$ . Given  $\boldsymbol{\tau} \in \mathbb{H}_0$ , let  $\mathbf{z} \in \mathbb{H}_0^1(\widetilde{\Omega})^2$  be the unique solution to the boundary value problem

$$(3.8) \quad \Delta \mathbf{z} = \begin{cases} \mathbf{curl}(\boldsymbol{\tau}), & \text{in } \Omega \\ 0, & \text{in } \widetilde{\Omega} \setminus \Omega \end{cases}, \quad \mathbf{z} = 0, \quad \text{in } \partial \widetilde{\Omega}.$$

Standard elliptic regularity results, states that the solution of (3.8) is such that  $\mathbf{z} \in \mathbb{H}^2(\Omega)^2$  and the estimate

$$\|\mathbf{z}\|_{2,\Omega} \lesssim \|\mathbf{curl}(\boldsymbol{\tau})\|_{0,\Omega},$$

where the hidden constant depends on the domain, holds. Note that  $\mathbf{curl}(\mathbf{z}) \in \mathbb{H}^1(\Omega)$  and  $\mathbf{curl}(\mathbf{curl}(\mathbf{z})) = \Delta \mathbf{z} = \mathbf{curl}(\boldsymbol{\tau})$  in  $\Omega$ . Moreover, we have

$$(3.9) \quad \|\mathbf{curl}(\mathbf{z})\|_{1,\Omega} \leq \|\mathbf{z}\|_{2,\Omega} \leq \|\mathbf{curl}(\boldsymbol{\tau})\|_{0,\Omega}.$$

Define the operator  $\mathcal{F}_h : \mathbb{H}_0 \rightarrow \mathbb{H}_{0,h}$  that maps  $\boldsymbol{\tau} \in \mathbb{H}_0$  into its  $\mathbb{H}_0$ -component of  $\mathbf{\Pi}_h^{\text{NED}(\epsilon)}(\mathbf{curl}(\mathbf{z}))$ , which is determined by the decomposition (2.5). More precisely, we have

$$\mathcal{F}_h \boldsymbol{\tau} := \mathbf{\Pi}_h^{\text{NED}(\epsilon)}(\mathbf{curl}(\mathbf{z})) - \left( \frac{1}{2|\Omega|} \int_{\Omega} \mathbf{\Pi}_h^{\text{NED}(\epsilon)}(\mathbf{curl}(\mathbf{z})) : \mathbb{J} \right) \mathbb{J}.$$

The above, together with (3.1), allows us to obtain

$$\mathbf{curl}(\mathcal{F}_h \boldsymbol{\tau}) = \mathbf{curl}(\mathbf{\Pi}_h^{\text{NED}(\epsilon)}(\mathbf{curl}(\mathbf{z}))) = \mathcal{R}_h(\mathbf{curl}(\mathbf{curl}(\mathbf{z}))) = \mathcal{R}_h \mathbf{curl}(\boldsymbol{\tau}).$$

Applying this equivalence, we deduce

$$(3.10) \quad b(\mathcal{F}_h \boldsymbol{\tau}, \mathbf{v}_h) = \int_{\Omega} \mathbf{v}_h \cdot \mathbf{curl}(\mathcal{F}_h \boldsymbol{\tau}) = \int_{\Omega} \mathbf{v}_h \cdot \mathcal{R}_h \mathbf{curl}(\boldsymbol{\tau}) = \int_{\Omega} \mathbf{v}_h \cdot \mathbf{curl}(\boldsymbol{\tau}) = b(\boldsymbol{\tau}, \mathbf{v}_h),$$

for all  $\boldsymbol{\tau} \in \mathbb{H}_0$  and for all  $\mathbf{v}_h \in \mathbf{Q}_h$ .

On the other hand, from the stability of the decomposition (2.5), (3.2) and (3.9), we have that

$$\begin{aligned} \|\mathcal{F}_h \boldsymbol{\tau}\|_{\mathbf{curl}, \Omega}^2 &\leq \|\boldsymbol{\Pi}_h^{\text{NED}(\ell)} \mathbf{curl}(\mathbf{z})\|_{0, \Omega}^2 + \|\mathbf{curl}(\boldsymbol{\Pi}_h^{\text{NED}(\ell)} \mathbf{curl}(\mathbf{z}))\|_{0, \Omega}^2 \\ &= \|\boldsymbol{\Pi}_h^{\text{NED}(\ell)} \mathbf{curl}(\mathbf{z})\|_{0, \Omega}^2 + \|\mathcal{R}_h \mathbf{curl}(\boldsymbol{\tau})\|_{0, \Omega}^2 \\ &\leq \|\mathbf{curl}(\mathbf{z}) - \boldsymbol{\Pi}_h^{\text{NED}(\ell)} \mathbf{curl}(\mathbf{z})\|_{0, \Omega}^2 + \|\mathbf{curl}(\mathbf{z})\|_{0, \Omega}^2 + \|\mathbf{curl}(\boldsymbol{\tau})\|_{0, \Omega}^2 \\ &\lesssim \|\mathbf{curl}(\boldsymbol{\tau})\|_{0, \Omega}^2, \end{aligned}$$

for all  $\boldsymbol{\tau} \in \mathbb{H}_0$ . Hence  $\mathcal{F}_h$  is uniformly bounded. This, along with (3.10) imply that  $\mathcal{F}_h$  is a Fortin operator. This concludes the proof.  $\square$

Let us introduce the discrete kernel of  $b(\cdot, \cdot)$ , defined by

$$\mathbb{V}_h := \{\boldsymbol{\tau}_h \in \mathbb{H}_{0,h} : b(\boldsymbol{\tau}_h, \mathbf{v}_h) = 0 \ \forall \mathbf{v}_h \in \mathbf{Q}_h\} = \{\boldsymbol{\tau}_h \in \mathbb{H}_{0,h} : \mathbf{curl}(\boldsymbol{\tau}_h) = \mathbf{0} \text{ in } \Omega\}.$$

It is easy to check  $a(\cdot, \cdot)$  is coercive in  $\mathbb{V}_h$ . Indeed, given  $\boldsymbol{\tau}_h \in \mathbb{H}_{0,h}$  we have

$$a(\boldsymbol{\tau}_h, \boldsymbol{\tau}_h) = \frac{1}{\mu} \|\boldsymbol{\tau}_h^r\|_{0, \Omega}^2 \geq \frac{C^2}{\mu} \|\boldsymbol{\tau}_h\|_{\mathbf{curl}, \Omega}^2,$$

where  $C$  is the constant of Lemma 2.1. With these ingredients at hand, we are in position to introduce the discrete solution operator associated to (3.5)–(3.6)

$$\mathbf{T}_h : \mathbf{Q} \rightarrow \mathbf{Q}_h, \quad \mathbf{f} \mapsto \mathbf{T}_h \mathbf{f} := \widehat{\mathbf{u}}_h,$$

where  $(\widehat{\boldsymbol{\sigma}}_h, \widehat{\mathbf{u}}_h) \in \mathbb{H}_{0,h} \times \mathbf{Q}_h$  is the solution of the following well posed source problem (see [10])

$$(3.11) \quad a(\widehat{\boldsymbol{\sigma}}_h, \boldsymbol{\tau}_h) + b(\boldsymbol{\tau}_h, \widehat{\mathbf{u}}_h) = 0 \quad \forall \boldsymbol{\tau}_h \in \mathbb{H}_{0,h},$$

$$(3.12) \quad b(\widehat{\boldsymbol{\sigma}}_h, \mathbf{v}_h) = -(\mathbf{f}, \mathbf{v}_h) \quad \forall \mathbf{v}_h \in \mathbf{Q}_h.$$

**4. Convergence and error estimates.** For the convergence analysis we take advantage of the compactness of the solution operator  $\mathbf{T}$  in order to obtain the convergence of  $\mathbf{T}_h$  to  $\mathbf{T}$  in norm, as  $h$  goes to zero. To do this task, we resort to the well established theory of [6] for compact operators.

We begin with the following approximation result

LEMMA 4.1. *Let  $\mathbf{f} \in \mathbf{Q}$ . Then, the following estimate holds*

$$\|(\mathbf{T} - \mathbf{T}_h) \mathbf{f}\|_{0, \Omega} \lesssim \|\widehat{\boldsymbol{\sigma}} - \boldsymbol{\Pi}_h^{\text{NED}(\ell)}(\widehat{\boldsymbol{\sigma}})\|_{0, \Omega} + \|\widehat{\mathbf{u}} - \mathcal{R}_h \widehat{\mathbf{u}}\|_{0, \Omega},$$

where the hidden constant are independent of  $h$  and  $\ell \in \{1, 2\}$ .

*Proof.* Let  $\mathbf{f} \in \mathbf{Q}$  be such that  $\mathbf{T} \mathbf{f} = \widehat{\mathbf{u}}$  and  $\mathbf{T}_h \mathbf{f} = \widehat{\mathbf{u}}_h$  where  $\widehat{\mathbf{u}}$  is the solution of (2.9)–(2.10) and  $\widehat{\mathbf{u}}_h$  is the solution of (3.11)–(3.12), we have

$$(4.1) \quad \|(\mathbf{T} - \mathbf{T}_h) \mathbf{f}\|_{0, \Omega} = \|\widehat{\mathbf{u}} - \widehat{\mathbf{u}}_h\|_{0, \Omega} \leq \|\widehat{\mathbf{u}} - \mathcal{R}_h \widehat{\mathbf{u}}\|_{0, \Omega} + \|\mathcal{R}_h \widehat{\mathbf{u}} - \widehat{\mathbf{u}}_h\|_{0, \Omega}.$$

Now our task is to control each of the terms on the right hand side of (4.1). We begin with the second term. Invoking the discrete inf-sup condition (3.7), and setting  $\mathbf{v}_h := \mathcal{R}_h \widehat{\mathbf{u}} - \widehat{\mathbf{u}}_h \in \mathbf{Q}_h^\mu$ , we obtain

$$\|\mathcal{R}_h \widehat{\mathbf{u}} - \widehat{\mathbf{u}}_h\|_{0, \Omega} \leq \frac{1}{\beta} \sup_{\mathbf{0} \neq \boldsymbol{\tau}_h \in \mathbb{H}_{0,h}} \frac{\int_{\Omega} \mathbf{curl}(\boldsymbol{\tau}_h) \cdot (\mathcal{R}_h \widehat{\mathbf{u}} - \widehat{\mathbf{u}}_h)}{\|\boldsymbol{\tau}_h\|_{\mathbf{curl}, \Omega}}.$$

Clearly  $\mathbf{curl}(\boldsymbol{\tau}_h) \in \mathbf{Q}_h$ . Then, since  $\mathcal{R}_h$  is the  $L^2(\Omega)$ -orthogonal projector, and invoking (2.9) and (3.11), straightforward calculations reveal

$$b(\boldsymbol{\tau}_h, \mathcal{R}_h \hat{\mathbf{u}} - \hat{\mathbf{u}}_h) = b(\boldsymbol{\tau}_h, \hat{\mathbf{u}}) - b(\boldsymbol{\tau}_h, \hat{\mathbf{u}}_h) = a(\hat{\boldsymbol{\sigma}}_h, \boldsymbol{\tau}_h) - a(\hat{\boldsymbol{\sigma}}, \boldsymbol{\tau}_h) \lesssim \|\hat{\boldsymbol{\sigma}}_h - \hat{\boldsymbol{\sigma}}\|_{0,\Omega} \|\boldsymbol{\tau}_h\|_{0,\Omega},$$

and

$$(4.2) \quad \|\mathcal{R}_h \hat{\mathbf{u}} - \hat{\mathbf{u}}_h\|_{0,\Omega} \lesssim \|\hat{\boldsymbol{\sigma}}_h - \hat{\boldsymbol{\sigma}}\|_{0,\Omega}.$$

From the triangle inequality we have

$$(4.3) \quad \|\hat{\boldsymbol{\sigma}} - \hat{\boldsymbol{\sigma}}_h\|_{0,\Omega} \leq \|\hat{\boldsymbol{\sigma}} - \boldsymbol{\Pi}_h^{\text{NED}^{(\ell)}}(\hat{\boldsymbol{\sigma}})\|_{0,\Omega} + \|\boldsymbol{\Pi}_h^{\text{NED}^{(\ell)}}(\hat{\boldsymbol{\sigma}}) - \hat{\boldsymbol{\sigma}}_h\|_{0,\Omega}$$

Now, using that  $\boldsymbol{\Pi}_h^{\text{NED}^{(\ell)}}(\hat{\boldsymbol{\sigma}}) - \hat{\boldsymbol{\sigma}}_h \in \mathbb{H}_{0,h}$ , the commuting diagram property (3.1), together with (2.10) and (3.12), we obtain  $\mathbf{curl}(\boldsymbol{\Pi}_h^{\text{NED}^{(\ell)}}(\hat{\boldsymbol{\sigma}})) = \mathcal{R}_h(\mathbf{curl}(\hat{\boldsymbol{\sigma}})) = \mathcal{R}_h(-\mathbf{f}) = \mathbf{curl}(\hat{\boldsymbol{\sigma}}_h)$ , implying directly that  $\mathbf{curl}(\boldsymbol{\Pi}_h^{\text{NED}^{(\ell)}}(\hat{\boldsymbol{\sigma}}) - \hat{\boldsymbol{\sigma}}_h) \in \mathbb{V}_h$ . Since  $a_0(\cdot, \cdot)$  is  $\mathbb{V}_h$ -elliptic, there exists  $\hat{\alpha} > 0$  such that

$$\hat{\alpha} \|\boldsymbol{\Pi}_h^{\text{NED}^{(\ell)}}(\hat{\boldsymbol{\sigma}}) - \hat{\boldsymbol{\sigma}}_h\|_{0,\Omega}^2 \lesssim \|\boldsymbol{\Pi}_h^{\text{NED}^{(\ell)}}(\hat{\boldsymbol{\sigma}}) - \hat{\boldsymbol{\sigma}}\|_{0,\Omega} \|\boldsymbol{\Pi}_h^{\text{NED}^{(\ell)}}(\hat{\boldsymbol{\sigma}}) - \hat{\boldsymbol{\sigma}}_h\|_{0,\Omega}.$$

These calculations imply that

$$(4.4) \quad \|\boldsymbol{\Pi}_h^{\text{NED}^{(\ell)}}(\hat{\boldsymbol{\sigma}}) - \hat{\boldsymbol{\sigma}}_h\|_{0,\Omega} \lesssim \|\boldsymbol{\Pi}_h^{\text{NED}^{(\ell)}}(\hat{\boldsymbol{\sigma}}) - \hat{\boldsymbol{\sigma}}\|_{0,\Omega}.$$

Then, from (4.1), (4.2), (4.3) and (4.4), we have

$$\|(\mathbf{T} - \mathbf{T}_h)\mathbf{f}\|_{0,\Omega} \lesssim \|\hat{\mathbf{u}} - \mathcal{R}_h \hat{\mathbf{u}}\|_{0,\Omega} + \|\boldsymbol{\Pi}_h^{\text{NED}^{(\ell)}}(\hat{\boldsymbol{\sigma}}) - \hat{\boldsymbol{\sigma}}\|_{0,\Omega}.$$

where the hidden constant is independent of  $h$ . This concludes the proof.  $\square$

It is important to remark that the previous result is valid for both  $\text{NED}_k^{(1)}$  and  $\text{NED}_{k+1}^{(2)}$  schemes, since the key ingredient to obtain the desired bound lies in the commutative diagram property that both elements satisfy. Now, with this result at hand, and following the proof of [28, Corollary 4.2] together with (3.2)–(3.4), for each finite element scheme, we have the following approximation result for the solution operators

$$(4.5) \quad \|(\mathbf{T} - \mathbf{T}_h)\mathbf{f}\|_{0,\Omega} \lesssim h^s \|\mathbf{f}\|_{0,\Omega},$$

where the hidden constant is independent of  $h$ .

Finally, all the previous results, together with the application of the theory in [25], state that our numerical methods are spurious free, as is stated in the following result.

**THEOREM 4.2.** *Let  $V \subset \mathbb{C}$  be an open set containing  $\text{sp}(\mathbf{T})$ . Then, there exists  $h_0 > 0$  such that  $\text{sp}(\mathbf{T}_h) \subset V$  for all  $h < h_0$ .*

**4.1. A priori error estimates.** Now our aim is to obtain error estimates for the eigenfunctions and eigenvalues. Let us remark that, according to (4.5), if  $\kappa \in (0, 1)$  is an isolated eigenvalue of  $\mathbf{T}$  with multiplicity  $m$ , and  $\mathcal{E}$  its associated eigenspace, then, there exist  $m$  eigenvalues  $\kappa_h^{(1)}, \dots, \kappa_h^{(m)}$  of  $\mathbf{T}_h$ , repeated according to their respective

multiplicities, which converge to  $\kappa$ . Let  $\mathcal{E}_h$  be the direct sum of their corresponding associated eigenspaces (see [25]) and let us define the *gap*  $\widehat{\delta}$  between two closed subspaces  $\mathcal{X}$  and  $\mathcal{Y}$  of  $L^2(\Omega)$  by

$$\widehat{\delta}(\mathcal{X}, \mathcal{Y}) := \max \{ \delta(\mathcal{X}, \mathcal{Y}), \delta(\mathcal{Y}, \mathcal{X}) \}, \text{ where } \delta(\mathcal{X}, \mathcal{Y}) := \sup_{\substack{x \in \mathcal{X} \\ \|x\|_{0,\Omega} = 1}} \left( \inf_{y \in \mathcal{Y}} \|x - y\|_{0,\Omega} \right).$$

With these definitions and hand, we derive the following error estimates for eigenfunctions and eigenvalues. Since the proof is direct from applying the results of [6, 11, 12], we do not incorporate further details.

**THEOREM 4.3.** *For  $k \geq 0$ , the following error estimates for the eigenfunctions and eigenvalues hold*

$$\widehat{\delta}(\mathcal{E}, \mathcal{E}_h) \lesssim h^{\min\{s, k+1\}} \quad \text{and} \quad |\mu - \mu_h(i)| \lesssim h^{\min\{s, k+1\}},$$

where the hidden constants are independent of  $h$ .

Now we improve the error estimate of Theorem 4.3 for the eigenvalues, showing that the order of convergence is in fact quadratic. This is contained in the following result.

**THEOREM 4.4.** *For  $k \geq 0$ , there exists a strictly positive constant  $h_0$  such that, for  $h < h_0$  there holds*

$$|\lambda - \lambda_h| \lesssim h^{2 \min\{s, k+1\}},$$

where the hidden constant is independent of  $h$ .

*Proof.* Let  $(\lambda, \boldsymbol{\sigma}, \mathbf{u})$  be the solution of problem (2.9)–(2.10), where its finite element approximation  $(\lambda_h, \boldsymbol{\sigma}_h, \mathbf{u}_h)$  corresponds to the solution of problem (3.5)–(3.6) with  $\|\mathbf{u}_h\|_{0,\Omega} = \|\mathbf{u}\|_{0,\Omega} = 1$ . Proceeding as in [16, Lemma 4], we deduce the following identity

$$\lambda - \lambda_h = \frac{1}{\mu} \|\boldsymbol{\sigma}^r - \boldsymbol{\sigma}_h^r\|_{0,\Omega}^2 - \lambda_h \|\mathbf{u} - \mathbf{u}_h\|_{0,\Omega}^2,$$

implying that

$$|\lambda - \lambda_h| \lesssim \|\boldsymbol{\sigma} - \boldsymbol{\sigma}_h\|_{0,\Omega}^2 + \|\mathbf{u} - \mathbf{u}_h\|_{0,\Omega}^2,$$

where the hidden constant is independent of  $h$ . The proof is complete using the same arguments of [28, Theorem 4.6].  $\square$

Since we have proved that our method does not introduce spurious eigenvalues, it is possible to conclude that for  $h$  small enough, except for  $\lambda_h$ , the rest of the eigenvalues of (3.5)–(3.6) are well separated from  $\lambda$ , as is stated in [13].

**PROPOSITION 4.5.** *Let us enumerate the eigenvalues of problems (3.5)–(3.6) and (2.3)–(2.4) in increasing order as follows:  $0 < \lambda_1 \leq \dots \leq \lambda_i \leq \dots$  and  $0 < \lambda_{h,1} \leq \dots \leq \lambda_{h,i} \leq \dots$ . Let us assume that  $\lambda_J$  is a simple eigenvalue of (3.5)–(3.6). Then, there exists  $h_0 > 0$  such that*

$$|\lambda_J - \lambda_{h,i}| \geq \frac{1}{2} \min_{j \neq J} |\lambda_j - \lambda_J| \quad \forall i \leq \dim \mathbb{H}_h, \quad i \neq J, \quad \forall h < h_0.$$

In what follows, we assume that  $\lambda$  is a simple eigenvalue and we normalize  $\mathbf{u}$  so that  $\|\mathbf{u}\|_{0,\Omega} = 1$ . Then, for all  $\mathcal{T}_h$ , there exists a solution  $(\lambda_h, \boldsymbol{\sigma}_h, \mathbf{u}_h)$  be a solution of problem (3.5)–(3.6) such that  $\lambda_h \rightarrow \lambda$  as  $h$  goes to zero and  $\|\mathbf{u}_h\|_{0,\Omega} = 1$ .

We conclude this section by presenting a summary of the approximation properties for functions and eigenvalues for the lowest order.

*Remark 4.6.* For  $k = 0$ , if  $(\lambda, \boldsymbol{\sigma}, \mathbf{u})$  is the solution of Problem (2.6)–(2.7) with  $\|\mathbf{u}\|_{0,\Omega} = 1$  and  $(\lambda_h, \boldsymbol{\sigma}_h, \mathbf{u}_h)$  is the solution of problem (3.5)–(3.6) with  $\|\mathbf{u}_h\|_{0,\Omega} = 1$ , then

$$\|\boldsymbol{\sigma} - \boldsymbol{\sigma}_h\|_{0,\Omega} + \|\mathbf{u} - \mathbf{u}_h\|_{0,\Omega} \lesssim h^s \quad \text{and} \quad |\lambda - \lambda_h| \lesssim \|\boldsymbol{\sigma} - \boldsymbol{\sigma}_h\|_{0,\Omega}^2 + \|\mathbf{u} - \mathbf{u}_h\|_{0,\Omega}^2,$$

where the hidden constant independent of  $h$ .

**5. A posteriori error analysis.** The aim of this section is to introduce and analysis of an a posteriori error estimator for our single eigenpair of the mixed eigenvalue problem. The main difficulty in the a posteriori error analysis for eigenvalue problems is to control the so called high order terms. To do this task, we adapt the results of [24] in order to obtain a superconvergence result and hence, prove the desire estimates for our estimator. The results presented in this section are limited to the lower order case  $k = 0$ , for which the required postprocessing operator is well defined.

**5.1. Properties of the mesh.** For  $T \in \mathcal{T}_h$ , let  $\mathcal{E}(T)$  be the set of its edges, and let  $\mathcal{E}_h$  be the set of all the edges of the triangulation  $\mathcal{T}_h$ . With these definitions at hand, we write  $\mathcal{E}_h := \mathcal{E}_h(\Omega) \cup \mathcal{E}_h(\partial\Omega)$ , where

$$\mathcal{E}_h(\Omega) := \{e \in \mathcal{E}_h : e \subseteq \Omega\} \quad \text{and} \quad \mathcal{E}_h(\partial\Omega) := \{e \in \mathcal{E}_h : e \subseteq \partial\Omega\}.$$

On the other hand, for each edge  $e \in \mathcal{E}_h$  we fix a unit normal vector  $\mathbf{n}_e$  to  $e$ . Moreover, given  $\boldsymbol{\tau} \in \mathbb{L}^2(\Omega)$  and  $e \in \mathcal{E}_h(\Omega)$ , we let  $[[\boldsymbol{\tau}]]$  be the corresponding normal jump across  $e$ , that is  $[[\boldsymbol{\tau}]] := (\boldsymbol{\tau}|_T - \boldsymbol{\tau}|_{T'})|_e \mathbf{n}_e$ , where  $T$  and  $T'$  are two elements of the triangulation with common edge  $e$ .

**5.2. Technical results.** We introduce some definitions and technical results that are necessary to perform the a posteriori analysis. We begin with the following result that is an adaptation of those presented in [14, Lemma 9, Lemma 10, Lemma 11]. For briefly we skip the details.

**COROLLARY 5.1.** *For the eigenfunction approximation  $\mathbf{u}_h$  of the eigenvalue problem (2.6)–(2.7), the following supercloseness result holds when the mesh size  $h$  is small enough,*

$$\|\mathbf{u}_h - \mathcal{R}_h \mathbf{u}\|_{0,\Omega} \lesssim h^s (\|\boldsymbol{\sigma} - \boldsymbol{\sigma}_h\|_{0,\Omega} + \|\mathbf{u} - \mathbf{u}_h\|_{0,\Omega}),$$

where the hidden constant is independent of  $h$ .

Let us introduce the following space

$$\mathbf{Y}_h := \{\mathbf{v} \in \mathbf{H}^1(\Omega)^2 : \mathbf{v} \in \mathbf{P}_1(T)^2, \quad \forall T \in \mathcal{T}_h\}.$$

Now, for each vertex  $z$  of the elements in  $\mathcal{T}_h$ , we define the patch  $\omega_z := \bigcup_{z \in T \in \mathcal{T}_h} T$ . To perform the a posteriori error analysis of our spectral problem, we introduce the so called the postprocessing operator (see [24] for instance) defined by  $\Theta_h : \mathbf{Q} \rightarrow \mathbf{Y}_h$  where, for the defined patch  $\omega_z$ , we fit a piecewise linear function in the average sense, for any  $\mathbf{v} \in \mathbf{Q}$  at the degrees of freedom of element integrations by

$$\Theta_h \mathbf{v}(z) := \sum_{T \in \omega_z} \frac{\int_T \mathbf{v} \, dx}{|\omega_z|}.$$

Here,  $|\omega_z|$  denotes the measure of the patch. Moreover,  $\Theta_h$  satisfies the following properties (see [24, Lemma 3.2, Theorem 3.3]).

LEMMA 5.2 (Properties of the postprocessing operator). *The operator  $\Theta_h$  defined above satisfies the following:*

1. For  $\mathbf{u} \in \mathbf{H}^{1+s}(\Omega)^2$  with  $s$  as in Theorem 2.2 and  $T \in \mathcal{T}_h$ , there holds

$$\|\Theta_h \mathbf{u} - \mathbf{u}\|_{0,\Omega} \lesssim h_T^{1+s} \|\mathbf{u}\|_{1+s,\Omega},$$

2.  $\Theta_h \mathcal{P}_h^0 \mathbf{v} = \Theta_h \mathbf{v}$ ,
3.  $\|\Theta_h \mathbf{v}\|_{0,\Omega} \lesssim \|\mathbf{v}\|_{0,\Omega}$  for all  $\mathbf{v} \in \mathbf{Q}$ ,

where the hidden constants are positive and independent of  $h$ .

The following result, proved in [24, Theorem 3.3] states a superconvergence property for  $\Theta_h$ .

LEMMA 5.3 (Superconvergence). *For  $h$  small enough, there holds*

$$\|\Theta_h \mathbf{u}_h - \mathbf{u}\|_{0,\Omega} \lesssim h^s (\|\boldsymbol{\rho} - \boldsymbol{\rho}_h\|_{0,\Omega} + \|\mathbf{u} - \mathbf{u}_h\|_{0,\Omega}) + \|\Theta_h \mathbf{u} - \mathbf{u}\|_{0,\Omega},$$

where the hidden constant is independent of  $h$ .

Let us introduce the bubble functions for two dimensional elements. Given  $T \in \mathcal{T}_h$  and  $e \in \mathcal{E}(T)$ , we let  $\psi_T$  and  $\psi_e$  be the usual triangle-bubble and edge-bubble functions, respectively (see [40, 41] for further details about these functions), which satisfy the following properties

1.  $\psi_T \in \mathbf{P}_3(T)$ ,  $\text{supp}(\psi_T) \subset T$ ,  $\psi_T = 0$  on  $\partial T$  and  $0 \leq \psi_T \leq 1$  in  $T$ ;
2.  $\psi_e|_T \in \mathbf{P}_2(T)$ ,  $\text{supp}(\psi_e) \subset \omega_e := \cup\{T' \in \mathcal{T}_h : e \in \mathcal{E}(T')\}$ ,  $\psi_e = 0$  on  $\partial T \setminus e$  and  $0 \leq \psi_e \leq 1$  in  $\omega_e$ .

The following results establish standard estimates for the bubble functions which will be essential for testing the efficiency of the residual estimator (see [40, Lemma 1.3]).

LEMMA 5.4 (Bubble function properties). *Given  $\ell \in \mathbb{N} \cup \{0\}$ , and for each  $T \in \mathcal{T}_h$  and  $e \in \mathcal{E}(T)$ , there hold*

$$\|\psi_T q\|_{0,T}^2 \leq \|q\|_{0,T}^2 \lesssim \|\psi_T^{1/2} q\|_{0,T}^2 \quad \forall q \in \mathbf{P}_\ell(T),$$

$$\|\psi_e L(p)\|_{0,e}^2 \leq \|p\|_{0,e}^2 \lesssim \|\psi_e^{1/2} p\|_{0,e}^2 \quad \forall p \in \mathbf{P}_\ell(e),$$

and

$$h_e \|p\|_{0,e}^2 \lesssim \|\psi_e^{1/2} L(p)\|_{0,T}^2 \lesssim h_e \|p\|_{0,e}^2 \quad \forall p \in \mathbf{P}_\ell(e),$$

where  $L : C(e) \rightarrow C(T)$  with  $L(p) \in \mathbf{P}_k(T)$  and  $L(p)|_e = p$  for all  $p \in \mathbf{P}_k(e)$ , and the hidden constants depend on  $k$  and the shape regularity of the triangulation.

Also, we require the following technical result (see [15, Theorem 3.2.6]).

LEMMA 5.5 (Inverse inequality). *Let  $l, m \in \mathbb{N} \cup \{0\}$  such that  $l \leq m$ . Then, for each  $T \in \mathcal{T}_h$  there holds*

$$|q|_{m,T} \lesssim h_T^{l-m} |q|_{l,T} \quad \forall q \in \mathbf{P}_k(T),$$

where the hidden constant depends on  $k, l, m$  and the shape regularity of the triangulations.

Finally, we will make use of the well known Clément interpolation operator  $I_h : \mathbf{H}^1(\Omega) \rightarrow C_I$ , where  $C_I := \{v \in \mathcal{C}(\Omega) : v|_T \in \mathbf{P}_1(T) \quad \forall T \in \mathcal{T}_h\}$ .

The following auxiliary results, available in [19], are necessary in our forthcoming analysis.



LEMMA 5.6. *For all  $v \in H^1(\Omega)$  there holds*

$$\|v - I_h v\|_{0,T} \lesssim h_T \|v\|_{1,\omega_T}, \quad \|v - I_h v\|_{0,e} \lesssim h_e^{1/2} \|v\|_{1,\omega_e},$$

for all  $T \in \mathcal{T}_h$  and for all  $e \in \mathcal{E}_h$ , where the hidden constants are independent of  $h$ , the set  $\omega_T$  is defined by

$$\omega_T := \{T' \in \mathcal{T}_h : T' \text{ and } T \text{ share an edge}\},$$

and  $\omega_e := \{T' \in \mathcal{T}_h : e \in \mathcal{E}_{T'}\}$ .

**5.3. The local and global estimators.** We are now in position to introduce our local estimators for the spectral problem (3.5)–(3.6).

The proposed estimator is of residual type, and our goal is to prove that is reliable and efficient. In what follows, let  $(\lambda_h, \boldsymbol{\sigma}_h, \mathbf{u}_h) \in \mathbb{R} \times \mathbb{H}_{0,h} \times \mathbf{Q}_h$  be the solution of (3.5)–(3.6). Now, for each  $T \in \mathcal{T}_h$  we define the local error indicator  $\eta_T$  as follows

$$(5.1) \quad \eta_T^2 := \|\Theta_h \mathbf{u}_h - \mathbf{u}_h\|_{0,T}^2 + h_T^2 \left\| \mathbf{curl}(\mathbf{u}_h) - \frac{1}{\mu} \boldsymbol{\sigma}_h^r \right\|_{0,T}^2 + h_T^2 \left\| \mathbf{div} \left( \frac{1}{\mu} \boldsymbol{\sigma}_h^r \right) \right\|_{0,T}^2 \\ + \sum_{e \in \mathcal{E}(T) \cap \mathcal{E}_h(\Omega)} h_e \left\| \left[ \frac{1}{\mu} \boldsymbol{\sigma}_h^r \right] \right\|_{0,e}^2 + \sum_{e \in \mathcal{E}(T) \cap \mathcal{E}_h(\partial\Omega)} h_e \left\| \frac{1}{\mu} \boldsymbol{\sigma}_h^r \mathbf{n}_e \right\|_{0,e}^2,$$

and the respective global estimator is defined by

$$(5.2) \quad \eta := \left\{ \sum_{T \in \mathcal{T}_h} \eta_T^2 \right\}^{1/2}.$$

**5.4. Reliability.** In this section we provide an upper bound for the proposed estimator (5.2). We begin by proving the following technical estimate.

LEMMA 5.7. *Let  $(\lambda, \boldsymbol{\sigma}, \mathbf{u}) \in \mathbb{R} \times \mathbb{H}_0 \times \mathbf{Q}$  be the solution of (2.6)–(2.7) and let  $(\lambda_h, \boldsymbol{\sigma}_h, \mathbf{u}_h) \in \mathbb{R} \times \mathbb{H}_{0,h} \times \mathbf{Q}_h$  be its finite element approximation, given as the solution of (3.5)–(3.6). Then, for all  $\boldsymbol{\tau} \in \mathbb{H}_0$ , we have.*

$$(5.3) \quad \|\boldsymbol{\sigma} - \boldsymbol{\sigma}_h\|_{\mathbf{curl},\Omega} + \|\mathbf{u} - \mathbf{u}_h\|_{0,\Omega} \lesssim \sup_{\substack{\boldsymbol{\tau} \in \mathbb{H}_0 \\ \boldsymbol{\tau} \neq \mathbf{0}}} \frac{-a(\boldsymbol{\sigma}_h, \boldsymbol{\tau}) - b(\boldsymbol{\tau}, \mathbf{u}_h)}{\|\boldsymbol{\tau}\|_{\mathbf{div},\Omega}} \\ + \underbrace{|\lambda_h - \lambda| + \|\mathbf{u} - \Theta_h \mathbf{u}_h\|_{0,\Omega} + \|\Theta_h \mathbf{u}_h - \mathbf{u}_h\|_{0,\Omega}}_{h.o.t},$$

where the hidden constant is independent of  $h$ .

*Proof.* Applying the inf-sup condition (2.11) on the errors  $\boldsymbol{\sigma} - \boldsymbol{\sigma}_h$  and  $\mathbf{u} - \mathbf{u}_h$  we have that that

$$\|(\boldsymbol{\sigma} - \boldsymbol{\sigma}_h, \mathbf{u} - \mathbf{u}_h)\|_{\mathbb{H}_0 \times \mathbf{Q}} \lesssim \sup_{\substack{(\boldsymbol{\tau}, \mathbf{v}) \in \mathbb{H}_0 \times \mathbf{Q} \\ (\boldsymbol{\tau}, \mathbf{v}) \neq \mathbf{0}}} \frac{a(\boldsymbol{\sigma} - \boldsymbol{\sigma}_h, \boldsymbol{\tau}) + b(\boldsymbol{\tau}, \mathbf{u} - \mathbf{u}_h) + b(\boldsymbol{\sigma} - \boldsymbol{\sigma}_h, \mathbf{v})}{\|(\boldsymbol{\tau}, \mathbf{v})\|_{\mathbb{H}_0 \times \mathbf{Q}}} \\ \lesssim \sup_{\substack{\boldsymbol{\tau} \in \mathbb{H}_0 \\ \boldsymbol{\tau} \neq \mathbf{0}}} \frac{-a(\boldsymbol{\sigma}_h, \boldsymbol{\tau}) - b(\boldsymbol{\tau}, \mathbf{u}_h)}{\|\boldsymbol{\tau}\|_{\mathbf{curl},\Omega}} + \sup_{\substack{\mathbf{v} \in \mathbf{Q} \\ \mathbf{v} \neq \mathbf{0}}} \frac{b(\boldsymbol{\sigma} - \boldsymbol{\sigma}_h, \mathbf{v})}{\|\mathbf{v}\|_{0,\Omega}},$$

where we have used (2.6). Now, according to the definition of the bilinear operator  $b(\cdot, \cdot)$ , the equation (2.7) and that  $\mathbf{curl}(\boldsymbol{\sigma}_h) = -\lambda_h \mathbf{u}_h$ , and finally using the Cauchy–Schwarz inequality, we obtain

$$\begin{aligned} \sup_{\substack{\mathbf{v} \in \mathbf{Q} \\ \mathbf{v} \neq \mathbf{0}}} \frac{b(\boldsymbol{\sigma} - \boldsymbol{\sigma}_h, \mathbf{v})}{\|\mathbf{v}\|_{0,\Omega}} &\leq \|\lambda_h \mathbf{u}_h - \lambda \mathbf{u}\|_{0,\Omega} \leq |\lambda_h - \lambda| \|\mathbf{u}_h\|_{0,\Omega} + |\lambda| \|\mathbf{u} - \mathbf{u}_h\|_{0,\Omega} \\ &\leq |\lambda_h - \lambda| \|\mathbf{u}_h\|_{0,\Omega} + |\lambda| (\|\mathbf{u} - \Theta_h \mathbf{u}_h\|_{0,\Omega} + \|\Theta_h \mathbf{u}_h - \mathbf{u}_h\|_{0,\Omega}). \end{aligned}$$

Then, using the above estimate and recalling that  $\|\mathbf{u}_h\|_{0,\Omega} = 1$  we have

$$\begin{aligned} \|\boldsymbol{\sigma} - \boldsymbol{\sigma}_h\|_{\mathbf{curl},\Omega} + \|\mathbf{u} - \mathbf{u}_h\|_{0,\Omega} &\lesssim \sup_{\substack{\boldsymbol{\tau} \in \mathbb{H}_0 \\ \boldsymbol{\tau} \neq \mathbf{0}}} \frac{-a(\boldsymbol{\sigma}_h, \boldsymbol{\tau}) - b(\boldsymbol{\tau}, \mathbf{u}_h)}{\|\boldsymbol{\tau}\|_{\mathbf{curl},\Omega}} \\ &\quad + \underbrace{|\lambda_h - \lambda| + \|\mathbf{u} - \Theta_h \mathbf{u}_h\|_{0,\Omega} + \|\Theta_h \mathbf{u}_h - \mathbf{u}_h\|_{0,\Omega}}_{\text{h.o.t}}. \end{aligned}$$

This concludes the proof.  $\square$

*Remark 5.8.* We note that, thanks to Lemmas 4.6, 5.2 and 5.3, the estimate for the high order term

$$\text{h.o.t} \leq Ch^s (\|\boldsymbol{\sigma} - \boldsymbol{\sigma}_h\|_{0,\Omega} + \|\mathbf{u} - \mathbf{u}_h\|_{0,\Omega}) + \|\mathbf{u} - \Theta_h \mathbf{u}\|_{0,\Omega} \lesssim h^{2s},$$

holds, where the constant  $C$  is uniform on  $h$ .

Our next goal is to bound the supremum in Lemma 5.7. To do this task, let  $\boldsymbol{\tau} \in \mathbb{H}_0$ , we proceed as in the proof of Lemma 3.2, and let  $\mathbf{z} \in \mathbb{H}_0^1(\tilde{\Omega})^2$  be the unique weak solution of the boundary value problem (3.8), where  $\tilde{\Omega}$  is a bounded convex polygonal domain containing  $\bar{\Omega}$ . Since  $\mathbf{curl}(\boldsymbol{\tau} - \mathbf{curl}(\mathbf{z})) = 0$  in  $\Omega$ , and  $\Omega$  is connected, there exists  $\boldsymbol{\varphi} := (\varphi_1, \varphi_2) \in \mathbb{H}^1(\Omega)^2$ , with  $\int_{\Omega} \varphi_1 = \int_{\Omega} \varphi_2 = 0$ , such that  $\boldsymbol{\tau} = \nabla \boldsymbol{\varphi} + \mathbf{curl}(\mathbf{z})$ , and we have

$$(5.4) \quad \|\mathbf{z}\|_{2,\Omega} + \|\boldsymbol{\varphi}\|_{1,\Omega} \lesssim \|\boldsymbol{\tau}\|_{\mathbf{curl},\Omega}.$$

Now, we let  $\boldsymbol{\varphi}_h := (I_h(\varphi_1), I_h(\varphi_2))$  and define  $\boldsymbol{\tau}_h \in \mathbb{H}_h$  as

$$\boldsymbol{\tau}_h := \nabla \boldsymbol{\varphi}_h + \mathbf{\Pi}_h^{\text{NED}^{(\epsilon)}}(\mathbf{curl}(\mathbf{z})) - d_h \mathbb{J},$$

where  $\mathbf{\Pi}_h^{\text{NED}^{(\epsilon)}}$  is the Nédelec interpolation operator that satisfies properties (3.1)–(3.4). The constant  $d_h$  is chosen in the following way

$$d_h := \frac{1}{2|\Omega|} \int_{\Omega} \boldsymbol{\tau}_h : \mathbb{J} = \frac{1}{2|\Omega|} \int_{\Omega} \left( \nabla \boldsymbol{\varphi}_h + \mathbf{\Pi}_h^{\text{NED}^{(\epsilon)}}(\mathbf{curl}(\mathbf{z})) \right) : \mathbb{J},$$

in order to admit that  $\boldsymbol{\tau}_h \in \mathbb{H}_{h,0}$ . Notice that we have used the fact that  $\boldsymbol{\tau} \in \mathbb{H}_0$  and its Helmholtz decomposition.

As a first step to bound the supremum appearing on the right hand side of (5.3), we note that for all  $\boldsymbol{\xi}_h \in \mathbb{H}_{0,h}$  and (3.5), we have

$$a(\boldsymbol{\sigma}_h, \boldsymbol{\xi}_h) + b(\boldsymbol{\xi}_h, \mathbf{u}_h) = 0.$$

On the other hand, let  $\boldsymbol{\xi} \in \mathbb{H}$  be such that

$$\boldsymbol{\xi} := \boldsymbol{\tau} - \boldsymbol{\tau}_h = \nabla \boldsymbol{\varphi} - \nabla \boldsymbol{\varphi}_h + \mathbf{curl}(\mathbf{z}) - \mathbf{\Pi}_h^{\text{NED}^{(\epsilon)}}(\mathbf{curl}(\mathbf{z})) + d_h \mathbb{J}.$$

Since  $\mathbf{curl}(\nabla\varphi - \nabla\varphi_h) = \mathbf{curl}(d_h\mathbb{J}) = 0$ , and invoking the commutative diagram property (3.1), identity above is written as follows

$$\mathbf{curl}(\boldsymbol{\xi}) = \mathbf{curl}(\mathbf{curl}(z) - \mathbf{\Pi}_h^{\text{NED}(\ell)}(\mathbf{curl}(z))) = \mathbf{curl}(\mathbf{curl}(z)) - \mathcal{R}_h(\mathbf{curl}(\mathbf{curl}(z))).$$

Now, since  $\mathcal{R}_h$  is the  $L^2(\Omega)$ -orthogonal projector, we have that  $b(\boldsymbol{\xi}, \mathbf{u}_h) = 0$ . Therefore, from the fact that  $\boldsymbol{\sigma}_h \in \mathbb{H}_{0,h}$  we obtain the following identity

$$- [a(\boldsymbol{\sigma}_h, \boldsymbol{\tau}) + b(\boldsymbol{\tau}, \mathbf{u}_h)] = - [a(\boldsymbol{\sigma}_h, \boldsymbol{\xi}) + b(\boldsymbol{\xi}, \mathbf{u}_h)] = -a(\boldsymbol{\sigma}_h, \boldsymbol{\xi}).$$

Now, invoking the definition of  $\boldsymbol{\xi}$  and that  $a(\boldsymbol{\sigma}_h, d_h\mathbb{J}) = d_h a(\boldsymbol{\sigma}_h, \mathbb{J}) = 0$  we obtain (5.5)

$$- [a(\boldsymbol{\sigma}_h, \boldsymbol{\tau}) + b(\boldsymbol{\tau}, \mathbf{u}_h)] = \underbrace{-a(\boldsymbol{\sigma}_h, \nabla(\varphi - \varphi_h))}_{\mathfrak{T}_1} + \underbrace{-a(\boldsymbol{\sigma}_h, \mathbf{curl}(z) - \mathbf{\Pi}_h^{\text{NED}(\ell)}(\mathbf{curl}(z)))}_{\mathfrak{T}_2},$$

where the terms  $\mathfrak{T}_1$  and  $\mathfrak{T}_2$  must be bounded. We begin with  $\mathfrak{T}_1$ .

LEMMA 5.9. *There exists certain constant independent of  $h$ , such that*

$$|\mathfrak{T}_1| \lesssim \left\{ \sum_{T \in \mathcal{T}_h} \eta_T^2 \right\}^{1/2} \|\boldsymbol{\tau}\|_{\mathbf{curl}, \Omega}.$$

*Proof.* First, we note that

$$\mathfrak{T}_1 = - \int_{\Omega} \frac{1}{\mu} \boldsymbol{\sigma}_h^r : (\nabla(\varphi - \varphi_h))^r = - \int_{\Omega} \frac{1}{\mu} \boldsymbol{\sigma}_h^r : \nabla(\varphi - \varphi_h).$$

Now, integrating by parts on each  $T \in \mathcal{T}_h$ , we obtain that

$$\begin{aligned} \mathfrak{T}_1 &= \int_{\Omega} -\frac{1}{\mu} \boldsymbol{\sigma}_h^r : \nabla(\varphi - \varphi_h) = \sum_{T \in \mathcal{T}_h} \int_T -\frac{1}{\mu} \boldsymbol{\sigma}_h^r : \nabla(\varphi - \varphi_h) \\ &= \sum_{T \in \mathcal{T}_h} \int_T \mathbf{div} \left( \frac{1}{\mu} \boldsymbol{\sigma}_h^r \right) \cdot (\varphi - \varphi_h) + \sum_{e \in \mathcal{E}_h(\Omega)} \int_e \left[ \frac{1}{\mu} \boldsymbol{\sigma}_h^r \right] \cdot (\varphi - \varphi_h) \\ &\quad + \sum_{e \in \mathcal{E}_h(\partial\Omega)} \int_e \frac{1}{\mu} \boldsymbol{\sigma}_h^r \mathbf{n}_e \cdot (\varphi - \varphi_h). \end{aligned}$$

Applying Cauchy-Schwarz inequality, recalling that  $\boldsymbol{\varphi}_h := (I_h(\varphi_1), I_h(\varphi_2))$ , and invoking the approximation properties presented in Lemma 5.6 and estimate (5.4), we have

$$\begin{aligned} |\mathfrak{T}_1| &\leq \sum_{T \in \mathcal{T}_h} h_T \left\| \mathbf{div} \left( \frac{1}{\mu} \boldsymbol{\sigma}_h^r \right) \right\|_{0,T} \|\boldsymbol{\varphi}\|_{1, \omega_T} + \sum_{e \in \mathcal{E}(T) \cap \mathcal{E}_h(\Omega)} h_e \left\| \left[ \frac{1}{\mu} \boldsymbol{\sigma}_h^r \right] \right\|_{0,e} \|\boldsymbol{\varphi}\|_{1, \omega_e} \\ &\quad + \sum_{e \in \mathcal{E}(T) \cap \mathcal{E}_h(\partial\Omega)} h_e \left\| \frac{1}{\mu} \boldsymbol{\sigma}_h^r \mathbf{n}_e \right\|_{0,e} \|\boldsymbol{\varphi}\|_{1, \omega_e} \lesssim \left\{ \sum_{T \in \mathcal{T}_h} \eta_T^2 \right\}^{1/2} \|\boldsymbol{\tau}\|_{\mathbf{curl}, \Omega}, \end{aligned}$$

where the hidden constant is independent of  $h$  and the discrete solution. This concludes the proof.  $\square$

The bound for  $\mathfrak{T}_2$  is contained in the following lemma.

LEMMA 5.10. *There exists certain constant, independent of  $h$ , such that*

$$|\mathfrak{I}_2| \lesssim \left\{ \sum_{T \in \mathcal{T}_h} \eta_T^2 \right\}^{1/2} \|\boldsymbol{\tau}\|_{\mathbf{curl}, \Omega}.$$

*Proof.* Using again that  $\mathbf{u}_h \in P_0(T)^2$ , for all  $T \in \mathcal{T}_h$ , we obtain

$$\int_{\Omega} \mathbf{curl}(\mathbf{u}_h) : \left( \mathbf{curl}(\mathbf{z}) - \mathbf{\Pi}_h^{\text{NED}(\ell)}(\mathbf{curl}(\mathbf{z})) \right) = 0.$$

Then, we obtain that

$$\begin{aligned} \mathfrak{I}_2 &= - \sum_{T \in \mathcal{T}_h} \left[ \int_T \left( \mathbf{curl}(\mathbf{u}_h) - \frac{1}{\mu} \boldsymbol{\sigma}_h^r \right) : \left( \mathbf{curl}(\mathbf{z}) - \mathbf{\Pi}_h^{\text{NED}(\ell)}(\mathbf{curl}(\mathbf{z})) \right) \right] \\ &\leq \sum_{T \in \mathcal{T}_h} \left\| \mathbf{curl}(\mathbf{u}_h) - \frac{1}{\mu} \boldsymbol{\sigma}_h^r \right\|_{0,T} \left\| \mathbf{curl}(\mathbf{z}) - \mathbf{\Pi}_h^{\text{NED}(\ell)}(\mathbf{curl}(\mathbf{z})) \right\|_{0,T} \\ &\lesssim \left\{ \sum_{T \in \mathcal{T}_h} h_T^2 \left\| \mathbf{curl}(\mathbf{u}_h) - \frac{1}{\mu} \boldsymbol{\sigma}_h^r \right\|_{0,T}^2 \right\}^{1/2} \|\mathbf{z}\|_{2,\Omega} \lesssim \left\{ \sum_{T \in \mathcal{T}_h} \eta_T^2 \right\}^{1/2} \|\boldsymbol{\tau}\|_{\mathbf{curl}, \Omega}, \end{aligned}$$

where we have used Cauchy-Schwarz inequality and the approximation properties (3.3) and (5.4). This concludes the proof.  $\square$

As a consequence of Lemma 4.6, Lemma 5.7, Remark 5.8, estimate (5.5), Lemmas 5.9 and 5.10, and the definition of the local estimator  $\eta_T$ , we have the following result

LEMMA 5.11. *Let  $(\lambda, \boldsymbol{\sigma}, \mathbf{u}) \in \mathbb{R} \times \mathbb{H}_0 \times \mathbf{Q}$  be the solution of (2.6)–(2.7) and let  $(\lambda_h, \boldsymbol{\sigma}_h, \mathbf{u}_h) \in \mathbb{R} \times \mathbb{H}_{0,h} \times \mathbf{Q}_h$  be its finite element approximation, given as the solution of (3.5)–(3.6). Then, there exists  $h_0$ , such that, for all  $h < h_0$ , there holds.*

$$\begin{aligned} \|\boldsymbol{\sigma} - \boldsymbol{\sigma}_h\|_{\mathbf{curl}, \Omega} + \|\mathbf{u} - \mathbf{u}_h\|_{0,\Omega} &\lesssim \left\{ \sum_{T \in \mathcal{T}_h} \eta_T^2 \right\}^{1/2} + \|\mathbf{u} - \Theta_h \mathbf{u}\|_{0,\Omega}, \\ |\lambda - \lambda_h| &\lesssim \sum_{T \in \mathcal{T}_h} \eta_T^2 + \|\mathbf{u} - \Theta_h \mathbf{u}\|_{0,\Omega}^2, \end{aligned}$$

where the hidden constants are independent of  $h$ .

**5.5. Efficiency.** The aim of this section is to obtain a lower bound for the local indicator (5.1). To do this task, we will apply the localization technique based in bubble functions, together with inverse inequalities. In order to present the material, the efficiency will be proved in several steps, where each one of these correspond to one of the terms of (5.1).

Now our task is to bound each of the contributions of  $\eta_T$  in (5.1). We begin with the term

$$h_T^2 \left\| \mathbf{curl}(\mathbf{u}_h) - \frac{1}{\mu} \boldsymbol{\sigma}_h^r \right\|_{0,T}^2.$$

Given an element  $T \in \mathcal{T}_h$ , and using that  $\mathbf{curl}(\mathbf{u}) = \boldsymbol{\sigma}^r / \mu$ , let us define  $\Upsilon_T := \mathbf{curl}(\mathbf{u}_h) - \boldsymbol{\sigma}_h^r / \mu$ . Then, invoking the properties of the bubble function  $\psi_T$  defined in

Lemma 5.4 we have

$$\begin{aligned} \|\Upsilon_T\|_{0,T}^2 &\lesssim \|\psi_T^{1/2}\Upsilon_T\|_{0,T}^2 = \int_T \psi_T \Upsilon_T : \left( \underline{\mathbf{curl}}(\mathbf{u}_h - \mathbf{u}) + \frac{1}{\mu}(\boldsymbol{\sigma}^r - \boldsymbol{\sigma}_h^r) \right) \\ &\lesssim \|\underline{\mathbf{curl}}(\psi_T \Upsilon_T)\|_{0,T} \|\mathbf{u} - \mathbf{u}_h\|_{0,T} + \|\psi_T \Upsilon_T\|_{0,T} \|\boldsymbol{\sigma} - \boldsymbol{\sigma}_h\|_{0,T} \\ &\lesssim h_T^{-1} \|\mathbf{u} - \mathbf{u}_h\|_{0,T} + \|\boldsymbol{\sigma} - \boldsymbol{\sigma}_h\|_{0,T} \|\Upsilon_T\|_{0,T}. \end{aligned}$$

Then we have that

$$(5.6) \quad h_T^2 \left\| \underline{\mathbf{curl}}(\mathbf{u}_h) - \frac{1}{\mu} \boldsymbol{\sigma}_h^r \right\|_{0,T}^2 \lesssim \|\mathbf{u} - \mathbf{u}_h\|_{0,T} + h_T^2 \|\boldsymbol{\sigma} - \boldsymbol{\sigma}_h\|_{0,T}.$$

Now we prove the following result.

LEMMA 5.12. *Let  $\boldsymbol{\tau}_h \in \mathbb{L}^2(\Omega)$  be a piecewise polynomial of degree  $k \geq 0$  on each  $T \in \mathcal{T}_h$  such that approximates  $\boldsymbol{\tau} \in \mathbb{L}^2(\Omega)$ , where  $\mathbf{div}(\boldsymbol{\tau}) = \mathbf{0}$  on each  $T \in \mathcal{T}_h$ . Then, there holds*

$$\|\mathbf{div}(\boldsymbol{\tau}_h)\|_{0,T} \lesssim h_T^{-1} \|\boldsymbol{\tau} - \boldsymbol{\tau}_h\|_{0,T} \quad \forall T \in \mathcal{T}_h,$$

where the hidden constant is independent of  $h$ .

*Proof.* From the bubble functions properties of Lemma 5.4, integrating by parts, using the fact that  $\psi_T = 0$  on  $\partial T$ , and applying Cauchy-Schwarz inequality, we obtain

$$\begin{aligned} \|\mathbf{div}(\boldsymbol{\tau}_h)\|_{0,T}^2 &\lesssim \|\psi_T^{1/2} \mathbf{div}(\boldsymbol{\tau}_h)\|_{0,T}^2 = \int_T \psi_T \mathbf{div}(\boldsymbol{\tau}_h) \cdot \mathbf{div}(\boldsymbol{\tau}_h - \boldsymbol{\tau}) \\ &= - \int_T \nabla(\psi_T \mathbf{div}(\boldsymbol{\tau}_h)) : (\boldsymbol{\tau}_h - \boldsymbol{\tau}) \lesssim \|\nabla(\psi_T \mathbf{div}(\boldsymbol{\tau}_h))\|_{0,T} \|\boldsymbol{\tau}_h - \boldsymbol{\tau}\|_{0,T} \\ &\lesssim h_T^{-1} \|\boldsymbol{\tau}_h - \boldsymbol{\tau}\|_{0,T} \|\psi_T \mathbf{div}(\boldsymbol{\tau}_h)\|_{0,T} \lesssim h_T^{-1} \|\boldsymbol{\tau}_h - \boldsymbol{\tau}\|_{0,T} \|\mathbf{div}(\boldsymbol{\tau}_h)\|_{0,T}. \end{aligned}$$

This conclude the proof.  $\square$

LEMMA 5.13. *Let  $\boldsymbol{\tau}_h \in \mathbb{L}^2(\Omega)$  be a piecewise polynomial of degree  $k \geq 0$  on each  $T \in \mathcal{T}_h$  such that approximates  $\boldsymbol{\tau} \in \mathbb{L}^2(\Omega)$ , where  $\mathbf{div}(\boldsymbol{\tau}) = \mathbf{0}$  on each  $T \in \mathcal{T}_h$ . Then, there holds*

$$\|\llbracket \boldsymbol{\tau}_h \rrbracket\|_{0,e} \lesssim h_e^{-1/2} \|\boldsymbol{\tau} - \boldsymbol{\tau}_h\|_{0,\omega_e} \quad \forall e \in \mathcal{E}_h,$$

where the hidden constant is independent of  $h$ .

*Proof.* Given an edge  $e \in \mathcal{E}_h$ , we denote by  $\mathbf{w}_h := \llbracket \boldsymbol{\tau}_h \rrbracket$  the corresponding jump of  $\boldsymbol{\tau}_h$ . Then, employing Lemma 5.4 and integrating by parts on each triangle, we obtain of  $\omega_e$ , we obtain

$$\begin{aligned} \|\mathbf{w}_h\|_{0,e}^2 &\lesssim \|\psi_e^{1/2} \mathbf{w}_h\|_{0,e}^2 = \|\psi_e^{1/2} L(\mathbf{w}_h)\|_{0,e}^2 = \int_e \psi_e L(\mathbf{w}_h) \cdot \llbracket \boldsymbol{\tau}_h \rrbracket \\ &= \int_{\omega_e} \mathbf{div}(\boldsymbol{\tau}_h) \cdot \psi_e L(\mathbf{w}_h) + \int_{\omega_e} \boldsymbol{\tau}_h : \nabla(\psi_e L(\mathbf{w}_h)). \end{aligned}$$

Now, since  $\llbracket \boldsymbol{\tau} \rrbracket = \mathbf{0}$ , we have

$$0 = \int_{\omega_e} \mathbf{div}(\boldsymbol{\tau}) \cdot \psi_e L(\mathbf{w}_h) + \int_{\omega_e} \boldsymbol{\tau} : \nabla(\psi_e L(\mathbf{w}_h)).$$

Thus, we have the following estimate

$$\begin{aligned} \|\mathbf{w}_h\|_{0,e}^2 &\lesssim \int_{\omega_e} \mathbf{div}(\boldsymbol{\tau}_h - \boldsymbol{\tau}) \cdot \psi_e L(\mathbf{w}_h) + \int_{\omega_e} (\boldsymbol{\tau}_h - \boldsymbol{\tau}) : \nabla(\psi_e L(\mathbf{w}_h)) \\ &\lesssim \|\mathbf{div}(\boldsymbol{\tau}_h)\|_{0,\omega_e} \|\psi_e L(\mathbf{w}_h)\|_{0,\omega_e} + \|\boldsymbol{\tau}_h - \boldsymbol{\tau}\|_{0,\omega_e} \|\nabla(\psi_e L(\mathbf{w}_h))\|_{0,\omega_e}. \end{aligned}$$

Now, applying Lemma 5.12 to each element of  $\omega_e$ , using that  $h_{T_e}^{-1} \leq h_e^{-1}$ , together with Lemmas 5.5 and 5.4, we obtain

$$\|\mathbf{w}_h\|_{0,e}^2 \lesssim h_e^{-1/2} \|\boldsymbol{\tau}_h - \boldsymbol{\tau}\|_{0,\omega_e} \|\mathbf{w}_h\|_{0,e}.$$

This concludes the proof.  $\square$

As a consequence of the above lemma, we have the following results

$$(5.7) \quad h_T^2 \left\| \mathbf{div} \left( \frac{1}{\mu} \boldsymbol{\sigma}_h^r \right) \right\|_{0,T}^2 \lesssim \|\boldsymbol{\sigma} - \boldsymbol{\sigma}_h\|_{0,T}^2, \quad \text{and} \quad h_e \left\| \left[ \frac{1}{\mu} \boldsymbol{\sigma}_h^r \right] \right\|_{0,e}^2 \lesssim \|\boldsymbol{\sigma} - \boldsymbol{\sigma}_h\|_{0,\omega_e}^2,$$

for all  $e \in \mathcal{E}_h(\Omega)$ , and the hidden constants are independent of  $h$ . Finally, for the term  $\|\Theta_h \mathbf{u}_h - \mathbf{u}_h\|_{0,T}^2$ , we add and subtract  $\Theta_h \mathbf{u}$  and  $\mathbf{u}$ , apply triangle inequality, and Lemma 5.2, leading to

$$(5.8) \quad \|\Theta_h \mathbf{u}_h - \mathbf{u}_h\|_{0,T}^2 \lesssim \|\mathbf{u} - \mathbf{u}_h\|_{0,T}^2 + \|\Theta_h \mathbf{u}_h - \Theta_h \mathbf{u}\|_{0,T}^2 + \|\Theta_h \mathbf{u} - \mathbf{u}\|_{0,T}^2.$$

Note that the last term of (5.8) is asymptotically negligible thanks to Lemma 5.2.

Gathering the previous results, namely (5.6)–(5.8), we are in a position to establish the efficiency  $\eta$ , which is stated in the following result.

**THEOREM 5.14 (Efficiency).** *The following estimate holds*

$$\eta^2 := \sum_{T \in \mathcal{T}_h} \eta_T^2 \lesssim \|\mathbf{u} - \mathbf{u}_h\|_{0,\Omega}^2 + \|\boldsymbol{\sigma} - \boldsymbol{\sigma}_h\|_{0,\Omega}^2 + h.o.t.,$$

where the hidden constant is independent of  $h$  and the discrete solution.

*Proof.* The proof is a consequence of (5.6)–(5.7) and Lemma 5.2.  $\square$

**Remark 5.15.** Through our paper, we have considered a formulation that eliminates the pressure, which can be recovered by a postprocess of the stress tensor. However, it is possible to consider a formulation in terms of the velocity, pressure and velocity as the one studied in [18] for the source problem. This leads to a more expensive finite element scheme, but flexible in the choice of finite elements. All the computations that we performed along our paper, can be replicated to this formulation that incorporates the pressure.

**6. Numerical experiments.** In this section we report some numerical tests in order to assess the performance of the proposed mixed element methods. We divide this section into two parts: in the first part, we are interested in the computation of the spectrum and the order of convergence for the eigenvalues. This is with the goal to verify the accuracy of the methods and compare the methods. The second part is related to assess the performance of the proposed a posteriori error estimator.

We have implemented the discrete eigenvalue problem in a FEniCS code [31, 3]. The rates of convergence have been computed with a least-square fitting.

With the computed results at hand, we compare the schemes that only differ on the  $\mathbb{H}(\mathbf{curl}, \Omega)$  finite element space. In what follows,  $N$  denotes the mesh resolution,

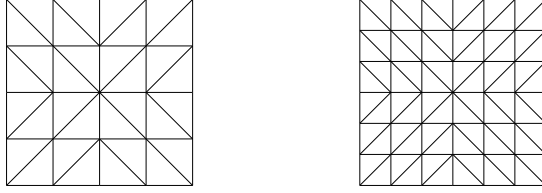


FIG. 1. Test 1. Examples of the meshes used in the unit square.

TABLE 1

Test 1. Lowest computed eigenvalues for polynomial degrees  $k = 0, 1, 2$  using the  $P_k^2\text{-NED}_k^{(1)}$  scheme.

$k$	$N = 20$	$N = 30$	$N = 40$	$N = 50$	Order	$\lambda_{extr}$	[32]
0	13.07172	13.07948	13.08235	13.08371	1.88	13.08636	13.086
	22.92407	22.98365	23.00442	23.01402	2.03	23.03084	23.031
	22.92407	22.98365	23.00442	23.01402	2.03	23.03084	23.031
	31.92158	31.99380	32.01930	32.03116	2.00	32.05232	32.053
	38.18216	38.37946	38.44657	38.47729	2.09	38.52901	38.532
1	13.08610	13.08615	13.08616	13.08617	3.56	13.08617	13.086
	23.03127	23.03112	23.03110	23.03110	4.60	23.03109	23.031
	23.03127	23.03112	23.03110	23.03110	4.60	23.03109	23.031
	32.05268	32.05242	32.05240	32.05239	5.59	32.05239	32.053
	38.53319	38.53172	38.53147	38.53141	4.04	38.53136	38.532
2	13.08617	13.08617	13.08617	13.08617	5.79	13.08617	13.086
	23.03109	23.03109	23.03109	23.03109	5.71	23.03109	23.031
	23.03109	23.03109	23.03109	23.03109	5.71	23.03109	23.031
	32.05238	32.05239	32.05239	32.05239	5.42	32.05239	32.053
	38.53137	38.53136	38.53136	38.53136	6.02	38.53136	38.532

with  $h \sim N^{-1}$ , and dof denotes the degrees of freedom, which will depend on the numerical scheme used.

In each test we plot selected eigenfunctions. The velocity field is recovered directly from solving the eigenproblem, whereas the pressure and vorticity are recovered in postprocessing by

$$p_h = -\frac{1}{2}(\boldsymbol{\sigma}_h : \mathbb{J}), \quad \underline{\text{curl}}(\mathbf{u}_h) = \frac{1}{\mu}(\boldsymbol{\sigma}_h + p_h \mathbb{J}).$$

Finally, we denote by  $P_k^2\text{-NED}_{\ell+k-1}^{(\ell)}$ , with  $\ell \in \{1, 2\}$  and  $k = 0, 1, 2$ , the numerical scheme using piecewise elements of order  $k$  to approximate  $\mathbf{u}$  and the Nédelec family  $\text{NED}_{\ell+k-1}^{(\ell)}$  of order  $\ell + k - 1$  to approximate  $\boldsymbol{\sigma}$ .

**6.1. Test 1: Square.** In this test we consider as computational domain the square  $\Omega := (-1, 1)^2$ , where the number of elements scales as  $2N^2$ . Examples of meshes used in the example are depicted in Figure 1. The convexity of this domain allows to obtain sufficiently smooth eigenfunctions. This implies that the convergence rates will be optimal, i.e., a behavior  $\mathcal{O}(h^{2(k+1)})$ , for  $k = 0, 1, 2$ , is expected.

In Table 1 we report the first five eigenvalues computed with the  $P_k^2\text{-NED}_k^{(1)}$  scheme, considering several refinement levels and  $k = 0, 1, 2$ . The column  $\lambda_{extr}$  shows extrapolated values, obtained with a least square fitting. The values are compared those of [32], where a similar experiment was performed.

For  $k = 0, 1$  the order of approximation is clearly  $\mathcal{O}(N^{-(k+1)})$ . Meanwhile for  $k = 2$  the computed convergence for the fourth eigenvalue is lower than optimal.

TABLE 2

Test 1. Lowest computed eigenvalues for polynomial degrees  $k=0, 1, 2$  using the  $P_k^2\text{-NED}_k^{(2)}$  scheme.

$k$	$N = 20$	$N = 30$	$N = 40$	$N = 50$	Order	$\lambda_{extr}$	[32]
0	13.18088	13.12837	13.10993	13.10138	2.02	13.08631	13.086
	23.32433	23.16178	23.10467	23.07821	2.02	23.03156	23.031
	23.32433	23.16178	23.10467	23.07821	2.02	23.03156	23.031
	32.61702	32.30485	32.19470	32.14355	2.00	32.05163	32.053
	39.35261	38.89728	38.73736	38.66325	2.02	38.53259	38.532
1	13.08642	13.08622	13.08618	13.08617	4.00	13.08617	13.086
	23.03240	23.03135	23.03118	23.03113	4.00	23.03109	23.031
	23.03240	23.03135	23.03118	23.03113	4.00	23.03109	23.031
	32.05619	32.05315	32.05263	32.05249	3.98	32.05239	32.053
	38.53707	38.53250	38.53172	38.53151	4.00	38.53136	38.532
2	13.08617	13.08617	13.08617	13.08617	6.13	13.08617	13.086
	23.03110	23.03109	23.03109	23.03109	6.06	23.03109	23.031
	23.03110	23.03109	23.03109	23.03109	6.06	23.03109	23.031
	32.05240	32.05239	32.05239	32.05239	6.04	32.05239	32.053
	38.53138	38.53136	38.53136	38.53136	6.00	38.53136	38.532

This is expected since for this numerical scheme, the computed eigenvalues on each refinement are very close to the extrapolated value, which affect the convergence rate. However, we observe that they match with those from the literature.

On the other hand, Table 2 shows the computed eigenvalues when using the  $P_k^2\text{-NED}_{k+1}^{(2)}$  scheme, where we observe that an optimal rate of convergence is reached for all choices of  $k$ . In this case, the deterioration of the convergence order for  $k = 2$  is not observed since the eigenvalues calculated with all possible decimal places always remain at a sufficient distance from the extrapolated value. This suggests a superior stability of the  $P_k^2\text{-NED}_{k+1}^{(2)}$  scheme at higher orders.

In Figure 2, a comparison of the error behavior between the two schemes is observed. We report curves for  $k = 1, 2$  since for  $k = 0$  the results are similar. Here, we consider the relative errors  $e_{\lambda_i}$ , for  $i = 1, \dots, 5$ , where

$$e_{\lambda_i} := \frac{|\lambda_{h_i} - \lambda_{extr_i}|}{|\lambda_{extr_i}|}.$$

Also, we denote by  $e_{\lambda_i}(\text{NED}_k^{(1)})$  and  $e_{\lambda_i}(\text{NED}_{k+1}^{(2)})$  the relative errors obtained using  $P_k^2\text{-NED}_k^{(1)}$  and  $P_k^2\text{-NED}_{k+1}^{(2)}$  schemes, respectively. It is clear that the slopes of the methods behaves like  $\mathcal{O}(h^{2(k+1)})$ .

For completeness, in Figure 3 we depict the velocity field and the postprocessed pressure on the square domain for the lowest computed eigenvalue. In Figure 4 we present the postprocessed vorticity components for the first computed eigenfunction.

**6.2. Test 2: Non-polygonal domain.** In this experiment we take a curved domain and approximate it by polygonal meshes. This leads to a variational crime, which will affect the order of convergence. The domain for this experiment is the unit circle  $\Omega := \{(x, y) \in \mathbb{R}^2 : x^2 + y^2 \leq 1\}$ , and in Figure 5 we show examples of the meshes we consider to approximate this domain. We recall that  $N$  represents the mesh resolution such that the number of elements is asymptotically  $6N^2$ .

First we present in Table 3 the results from approximating the eigenproblem using the  $P_k^2\text{-NED}_k^{(1)}$  scheme. It is observed that, for the case  $k = 0$  we have the desired



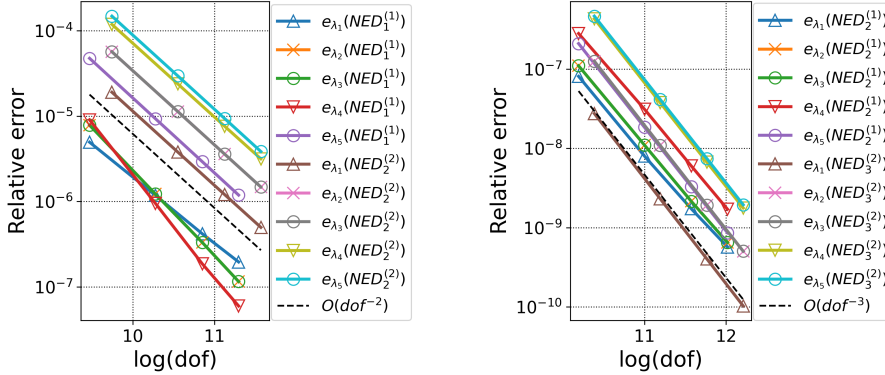


FIG. 2. Test 1. Comparison of the eigenvalues error curves in the square domain using  $P_k^2\text{-NED}_k^{(1)}$  and  $P_k^2\text{-NED}_{k+1}^{(2)}$ , for  $k = 1, 2$ .



FIG. 3. Test 1. Approximate velocity field  $\mathbf{u}_h$  (left) and postprocessed pressure  $p_h$  (right), corresponding to the first eigenvalue in the square domain.

convergence. However, for  $k > 0$  we observe that the convergence remains at  $\mathcal{O}(h^2) \simeq \mathcal{O}(\text{dof}^{-1})$ , showing explicitly the effect of variational crime. This is also reflected in Table 4, where despite applying the  $P_k^2\text{-NED}_k^{(2)}$  scheme, which contains more dofs, the convergence does not improve for  $k > 0$ . However, the results obtained are in good agreement with those predicted by theory. The results from using the  $P_k^2\text{-NED}_{k+1}^{(2)}$  scheme are described in Table 4, where similar rates of convergence are observed. We further explore the results by presenting Figure 6 and 7. In Figure 6 we can observe the velocity and postprocessed pressure for the fourth normal mode approximation, while the vorticity components calculated by postprocessing are observed in Figure 7.

**6.3. Test 3: Mixed boundary conditions.** The aim of the following test is to explore the performance of the proposed method in a more general eigenvalue problem. To do this task, we consider the the boundary  $\partial\Omega$  of our domain is separated into two section by  $\partial\Omega := \Gamma_D \cup \Gamma_N$ , where  $\Gamma_D$  and  $\Gamma_N$  represents the part of the boundary where we impose Dirichlet and Neumann boundary conditions, respectively. We assume that both  $\Gamma_D$  and  $\Gamma_N$  have positive measure. With these definitions at hand, the problem to consider is the following: Find  $\lambda \in \mathbb{R}$ , the stress  $\boldsymbol{\sigma}$ , the velocity  $\mathbf{u}$  and the pressure

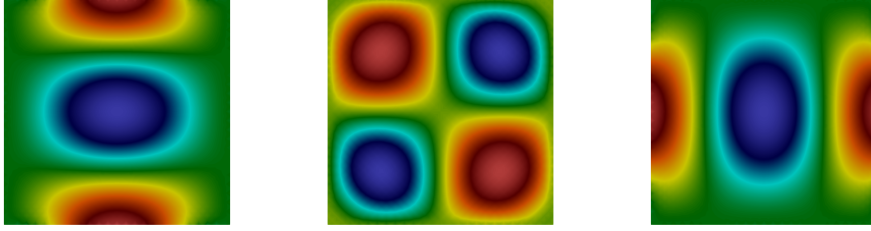


FIG. 4. Test 1. Postprocessed vorticity components  $\mathbf{curl}(\mathbf{u}_h)_{11}$  (left),  $\mathbf{curl}(\mathbf{u}_h)_{12}$  (center) and  $\mathbf{curl}(\mathbf{u}_h)_{22}$  (right) corresponding to the first eigenvalue in the square domain.

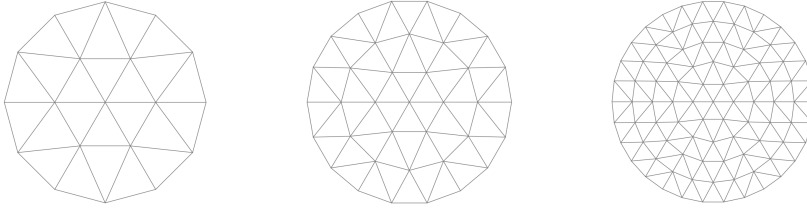


FIG. 5. Test 2. Example of meshes used in the circular domain.

TABLE 3

Test 2. Lowest computed eigenvalues for polynomial degrees  $k = 0, 1, 2$  using the  $P_k^2$ -NED $_k^{(1)}$  scheme.

$k$	$N = 20$	$N = 30$	$N = 40$	$N = 50$	Order	$\lambda_{extr}$	[26]
0	14.70187	14.69082	14.68695	14.68515	2.01	14.68198	14.68345
	26.39800	26.38501	26.38046	26.37835	2.01	26.37463	26.37840
	26.39800	26.38501	26.38046	26.37835	2.01	26.37463	26.37862
	40.73553	40.71969	40.71396	40.71128	1.93	40.70625	40.71434
	40.73553	40.71969	40.71396	40.71128	1.93	40.70625	40.71606
1	14.68868	14.68495	14.68364	14.68304	2.01	14.68197	14.68345
	26.38672	26.37998	26.37763	26.37654	2.02	26.37464	26.37840
	26.38672	26.37998	26.37763	26.37654	2.02	26.37464	26.37862
	40.72530	40.71477	40.71113	40.70944	2.03	40.70651	40.71434
	40.72530	40.71477	40.71113	40.70944	2.03	40.70651	40.71606
2	14.68871	14.68496	14.68365	14.68304	2.01	14.68361	14.68345
	26.38673	26.37999	26.37763	26.37654	2.01	26.37680	26.37840
	26.38673	26.37999	26.37763	26.37654	2.01	26.37680	26.37862
	40.72516	40.71476	40.71112	40.70944	2.01	40.70647	40.71434
	40.72516	40.71476	40.71112	40.70944	2.01	40.70647	40.71606



FIG. 6. Test 2. Approximate velocity field  $\mathbf{u}_h$  (left) and postprocessed pressure  $p_h$  (right), corresponding to the fourth eigenvalue in the unit circular domain.

TABLE 4

Test 2. Lowest computed eigenvalues for polynomial degrees  $k=0,1,2$  using the  $P_k^2\text{-NED}_{k+1}^{(2)}$  scheme.

$k$	$N = 20$	$N = 30$	$N = 40$	$N = 50$	Order	$\lambda_{extr}$	[26]
0	14.82469	14.71768	14.69784	14.69090	2.01	14.68199	14.68345
	26.77392	26.47427	26.41889	26.39951	2.02	26.37450	26.37840
	26.77392	26.47427	26.41889	26.39951	2.02	26.37450	26.37862
	41.56881	40.92423	40.80343	40.76105	2.01	40.70545	40.71434
	41.56881	40.92423	40.80343	40.76105	2.01	40.70545	40.71606
1	14.68873	14.68496	14.68365	14.68304	2.02	14.68198	14.68345
	26.38682	26.38000	26.37764	26.37655	2.03	26.37464	26.37840
	26.38682	26.38000	26.37764	26.37655	2.03	26.37464	26.37862
	40.72553	40.71483	40.71115	40.70945	2.05	40.70654	40.71434
	40.72553	40.71483	40.71115	40.70945	2.05	40.70654	40.71606
2	14.68874	14.68497	14.68365	14.68304	2.02	14.68198	14.68345
	26.38678	26.38000	26.37764	26.37655	2.02	26.37464	26.37840
	26.38678	26.38000	26.37764	26.37655	2.02	26.37464	26.37862
	40.72524	40.71478	40.71113	40.70945	2.01	40.70646	40.71434
	40.72524	40.71478	40.71113	40.70945	2.01	40.70646	40.71606

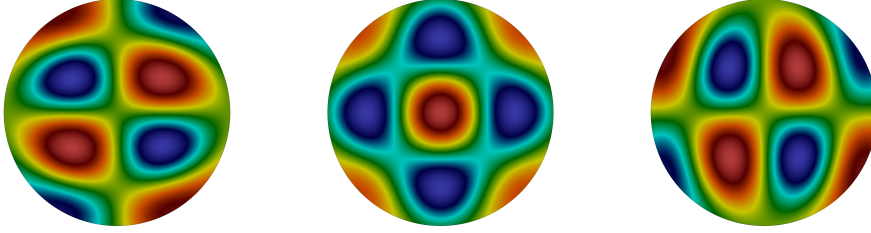


FIG. 7. Test 1. Postprocessed vorticity components  $\mathbf{curl}(\mathbf{u}_h)_{11}$  (left),  $\mathbf{curl}(\mathbf{u}_h)_{12}$  (center) and  $\mathbf{curl}(\mathbf{u}_h)_{22}$  (right) corresponding to the fourth eigenvalue in the circular domain.

$p$  such that

$$\left\{ \begin{array}{ll} \boldsymbol{\sigma} - \mu \mathbf{curl}(\mathbf{u}) - p\mathbb{J} = \mathbf{0} & \text{in } \Omega, \\ \mathbf{curl}(\boldsymbol{\sigma}) = -\lambda \mathbf{u} & \text{in } \Omega, \\ p = -\frac{1}{2}(\boldsymbol{\sigma} : \mathbb{J}) & \text{in } \Omega, \\ \mathbf{u} = \mathbf{0} & \text{on } \Gamma_D, \\ \boldsymbol{\sigma} \mathbf{s} = \mathbf{0} & \text{on } \Gamma_N, \end{array} \right.$$

where  $\mathbf{s}$  corresponds to the tangential component of the unitary vector on  $\Gamma_N$ . In what follows we will consider  $\Omega := (0, 1)^2$  as computational domain. For this square, we assume that the bottom is fixed and the rest of its sides are free of stress. We observe from Table 5 that the computed eigenvalues are accurately recovered with our both numerical schemes, with a clearly quadratic order of convergence. Moreover, our extrapolated values are close to those presented on [33] for an alternative formulation of the Stokes spectral problem. On the other hand, we present in Figures 8 and 9 plots of the velocity field, pressure and vorticity components associated to the third eigenfunction of the problem with mixed boundary.

**6.4. Test 4. A posteriori test on a non-convex domain.** We end our numerical test section with results for the proposed a posteriori estimator. To do this task, we focus on simple eigenvalues of the spectrum of  $\mathbf{T}$ . The computational domain for this test is  $\Omega := (-1, 1) \times (-1, 1) \setminus ((-1, 0) \times (-1, 0))$  and the only boundary

TABLE 5

Test 3. Lowest computed eigenvalues using the  $P_0^2\text{-NED}_0^{(1)}$ , and  $P_0^2\text{-NED}_1^{(2)}$ , schemes in the square domain with mixed boundary conditions.

scheme	$N = 20$	$N = 30$	$N = 40$	$N = 50$	Order	$\lambda_{extr}$	[33]
$P_0^2\text{-NED}_0^{(1)}$	2.46736	2.46738	2.46739	2.46739	2.14	2.46740	2.4674
	6.24652	6.26420	6.27066	6.27372	1.91	6.27952	6.2799
	15.16639	15.18837	15.19693	15.20112	1.74	15.21010	15.2090
	22.20329	22.20521	22.20584	22.20612	2.18	22.20657	22.2065
	26.84469	26.91450	26.92896	26.93579	1.92	26.94869	26.9479
$P_0^2\text{-NED}_1^{(2)}$	2.46824	2.46777	2.46761	2.46753	2.03	2.46740	2.4674
	6.28434	6.28163	6.28065	6.28019	1.95	6.27935	6.2799
	15.23974	15.22297	15.21701	15.21423	1.98	15.20917	15.2090
	22.27513	22.23705	22.22373	22.21756	2.03	22.20678	22.2065
	27.04797	26.99278	26.97339	26.96439	2.01	26.94835	26.9479

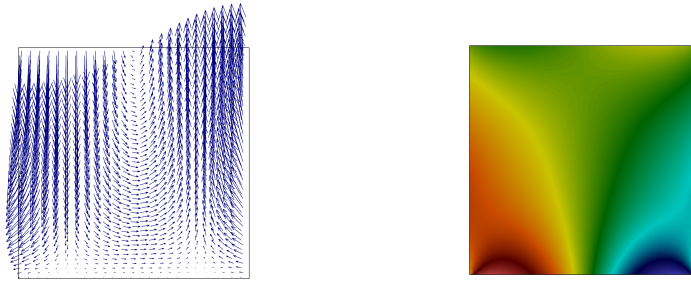


FIG. 8. Test 3. Approximate velocity field  $\mathbf{u}_h$  (left) and postprocessed pressure  $p_h$  (right), corresponding to the third eigenvalue in the square domain with mixed boundary conditions.

condition is  $\mathbf{u} = \mathbf{0}$ . Since the reentrant angle of this domain leads to a lack of regularity for some eigenfunctions associated to  $\mathbf{T}$ , our goal is to recover the optimal order of convergence with the proposed estimator. The initial mesh for this test is depicted in Figure 10.

It is well known that the regularity of the eigenfunctions in this geometry satisfy  $2r \geq 1.08$ , so that under uniform refinements, suboptimal error rates are expected since  $s \approx 2 \min\{r, k + 1\}$  (see, for instance [32, 28]). The extrapolated value for this experiment have been obtained through sufficiently fine meshing and least squares fitting. We choose  $\lambda_1 = 32.13183$  as an exact solution, which is in good agreement with the references above.

The adaptively refinement procedure is based on the blue-green marking strategy, consisting of refining the triangle  $T$  that satisfy

$$\eta_T \geq 0.5 \max_{T' \in \mathcal{T}_h} \eta_{T'}.$$

In Table 6 we observe the behavior of the estimator  $\eta$  defined in (5.2) when the families  $\text{NED}_0^{(1)}$  and  $\text{NED}_1^{(2)}$  are used, with 15 iterations of the adaptive refinement. Note that  $|\lambda_1 - \lambda_{1h}| \approx C \text{dof}^{-1.04} \approx Ch^{2.08}$ . We also note that the additional degrees of freedom of the  $P_0^2 - \text{NED}_1^{(2)}$  scheme allow the method to be more efficient in the sense that, the elements marked for refinement are fewer than those when using  $P_0^2 - \text{NED}_0^{(1)}$ . This is also observed in the intermediate meshes used in the adaptive algorithm shown in Figure 12. The column corresponding to the effectivity  $|\lambda_1 - \lambda_{1h}|/\eta^2$  shows that our estimator remains properly bounded above and below, away from zero.

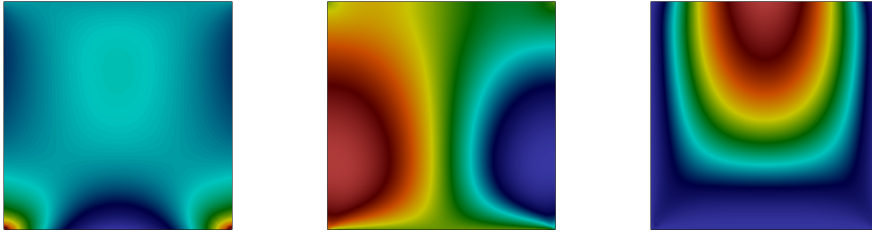


FIG. 9. *Test 3. Postprocessed vorticity components  $\mathbf{curl}(\mathbf{u}_h)_{11}$  (left),  $\mathbf{curl}(\mathbf{u}_h)_{12}$  (center) and  $\mathbf{curl}(\mathbf{u}_h)_{22}$  (right) corresponding to the third eigenvalue in the square domain with mixed boundary conditions.*

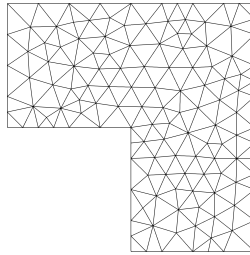


FIG. 10. *Test 4. Initial mesh on the L-shaped domain.*

A graphical description of these results can be seen in Figure 11, where we can observe the errors and the values of the estimator for each method. It is observed that the errors behave similar to  $\eta^2$ , i.e., they decay as  $\mathcal{O}(h^2)$ , so the efficiency and reliability are verified. Moreover, the plot includes a line with slope  $-1.0$ , which corresponds to the optimal order of convergence for the proposed schemes. The slopes of the lines obtained by a least squares fitting of the values computed with the adaptive scheme are  $-1.04$ .

#### REFERENCES

- [1] M. AINSWORTH AND J. T. ODEN, *A posteriori error estimation in finite element analysis*, Pure and Applied Mathematics (New York), Wiley-Interscience [John Wiley & Sons], New York, 2000, <https://doi.org/10.1002/9781118032824>.
- [2] A. AL-TAWHEEL, X. WANG, X. YE, AND S. ZHANG, *A stabilizer free weak Galerkin finite element method with supercloseness of order two*, Numer. Methods Partial Differential Equations, 37 (2021), pp. 1012–1029, <https://doi.org/10.1002/num.22564>.
- [3] M. S. ALNÆS, J. BLECHTA, J. HAKE, A. JOHANSSON, B. KEHLET, A. LOGG, C. RICHARDSON, J. RING, M. E. ROGNES, AND G. N. WELLS, *The fenics project version 1.5*, Archive of Numerical Software, 3 (2015), <https://doi.org/10.11588/ans.2015.100.20553>.
- [4] P. F. ANTONIETTI, L. BEIRÃO DA VEIGA, D. MORA, AND M. VERANI, *A stream virtual element formulation of the Stokes problem on polygonal meshes*, SIAM J. Numer. Anal., 52 (2014), pp. 386–404, <https://doi.org/10.1137/13091141X>.
- [5] M. G. ARMENTANO AND V. MORENO, *A posteriori error estimates of stabilized low-order mixed finite elements for the Stokes eigenvalue problem*, J. Comput. Appl. Math., 269 (2014), pp. 132–149, <https://doi.org/10.1016/j.cam.2014.03.027>.
- [6] I. BABUŠKA AND J. OSBORN, *Handbook of numerical analysis. Vol. II*, (1991), pp. x+928. Finite element methods. Part 1.
- [7] T. P. BARRIOS, E. M. BEHRENS, AND R. BUSTINZA, *An a posteriori error estimate for a dual mixed method applied to Stokes system with non-null source terms*, Adv. Comput. Math., 47 (2021), pp. Paper No. 77, 34, <https://doi.org/10.1007/s10444-021-09906-2>.
- [8] L. BEIRÃO DA VEIGA, F. DASSI, AND G. VACCA, *The Stokes complex for virtual elements*

TABLE 6

Test 4. Computed eigenfunction  $\lambda_{1h}$ , error and effectivity indexes using the  $P_0^2\text{-NED}_0^{(1)}$  and  $P_0^2\text{-NED}_1^{(2)}$  schemes with adaptively refinements.

scheme	dof	$\lambda_{1h}$	$ \lambda_1 - \lambda_{1h} $	$\eta^2$	$ \lambda_1 - \lambda_{1h} /\eta^2$
$P_0^2\text{-NED}_0^{(1)}$	1181	30.19673	1.93509e+00	2.50851e+01	7.71413e-02
	1399	31.01101	1.12082e+00	2.06562e+01	5.42608e-02
	1975	31.33653	7.95304e-01	1.48616e+01	5.35140e-02
	2919	31.60707	5.24757e-01	1.01735e+01	5.15805e-02
	4471	31.75965	3.72184e-01	7.04846e+00	5.28036e-02
	6561	31.88079	2.51042e-01	4.92335e+00	5.09900e-02
	10023	31.98109	1.50742e-01	3.31763e+00	4.54366e-02
	14067	32.00944	1.22386e-01	2.38015e+00	5.14196e-02
	21599	32.05984	7.19859e-02	1.59321e+00	4.51830e-02
	31619	32.08211	4.97245e-02	1.09533e+00	4.53967e-02
	45401	32.09712	3.47087e-02	7.61922e-01	4.55541e-02
	66797	32.10917	2.26548e-02	5.21796e-01	4.34171e-02
	97183	32.11631	1.55191e-02	3.59593e-01	4.31573e-02
	143721	32.12159	1.02378e-02	2.44116e-01	4.19381e-02
204461	32.12516	6.66500e-03	1.70746e-01	3.90346e-02	
	Order $\lambda_1$	$\mathcal{O}(\text{dof}^{-1.04})$ 32.13183			
$P_0^2\text{-NED}_1^{(2)}$	1907	33.05942	9.27595e-01	1.44740e+01	6.40871e-02
	2103	33.23013	1.09830e+00	8.41858e+00	1.30462e-01
	2347	33.29788	1.16605e+00	5.44523e+00	2.14142e-01
	2575	33.34447	1.21264e+00	4.17494e+00	2.90457e-01
	2893	33.31662	1.18480e+00	3.29619e+00	3.59443e-01
	3609	32.96793	8.36099e-01	2.16033e+00	3.87023e-01
	4677	32.66458	5.32752e-01	1.36450e+00	3.90438e-01
	5559	32.58139	4.49556e-01	1.06559e+00	4.21885e-01
	8325	32.41385	2.82018e-01	6.42697e-01	4.38804e-01
	11651	32.34513	2.13299e-01	4.04288e-01	5.27590e-01
	16179	32.27964	1.47810e-01	2.59997e-01	5.68505e-01
	21025	32.24409	1.12260e-01	1.86314e-01	6.02532e-01
	31091	32.20603	7.42023e-02	1.14587e-01	6.47564e-01
	40873	32.18761	5.57772e-02	8.11620e-02	6.87233e-01
57171	32.17095	3.91252e-02	5.45027e-02	7.17859e-01	
	Order $\lambda_1$	$\mathcal{O}(\text{dof}^{-1.04})$ 32.13183			

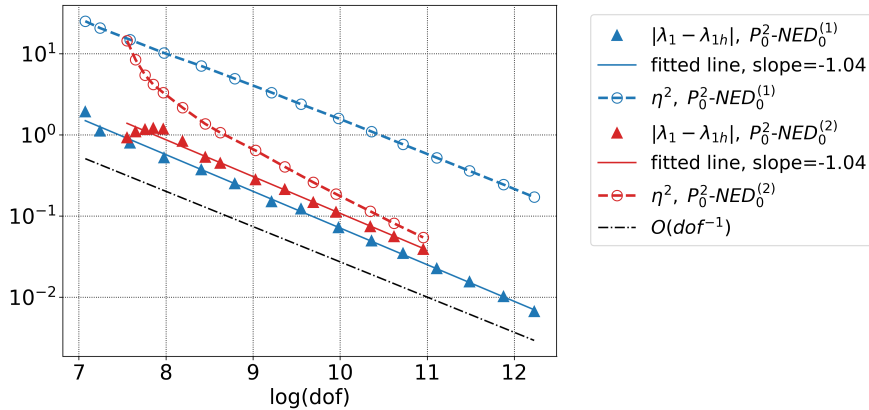


FIG. 11. Test 4. Comparison between error, estimators and fit lines in the adaptive refinement using the lowest order  $\text{NED}_0^{(1)}$  and  $\text{NED}_1^{(2)}$  families.



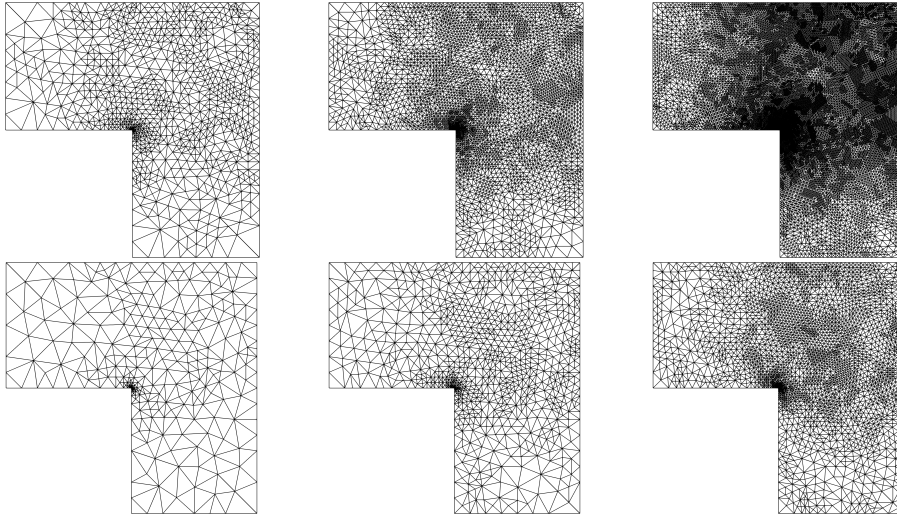


FIG. 12. *Test 4. Adapted meshes associated to estimator  $\eta$  in the seventh, eleventh and last iteration. Top row:  $P_0\text{-NED}_0^{(1)}$  scheme with 10023, 45401 and 204461 degrees of freedom. Bottom row:  $P_0\text{-NED}_0^{(2)}$  with 4677, 16179 and 57171 degrees of freedom.*

- in three dimensions, *Math. Models Methods Appl. Sci.*, 30 (2020), pp. 477–512, <https://doi.org/10.1142/S0218202520500128>.
- [9] L. BEIRÃO DA VEIGA, C. LOVADINA, AND G. VACCA, *Divergence free virtual elements for the Stokes problem on polygonal meshes*, *ESAIM Math. Model. Numer. Anal.*, 51 (2017), pp. 509–535, <https://doi.org/10.1051/m2an/2016032>.
- [10] D. BOFFI, F. BREZZI, AND M. FORTIN, *Mixed finite element methods and applications*, vol. 44 of Springer Series in Computational Mathematics, Springer, Heidelberg, 2013, <https://doi.org/10.1007/978-3-642-36519-5>.
- [11] D. BOFFI, F. BREZZI, AND L. GASTALDI, *On the convergence of eigenvalues for mixed formulations*, vol. 25, 1997, pp. 131–154 (1998). Dedicated to Ennio De Giorgi.
- [12] D. BOFFI, F. BREZZI, AND L. GASTALDI, *On the problem of spurious eigenvalues in the approximation of linear elliptic problems in mixed form*, *Math. Comp.*, 69 (2000), pp. 121–140, <https://doi.org/10.1090/S0025-5718-99-01072-8>.
- [13] D. BOFFI, D. GALLISTL, F. GARDINI, AND L. GASTALDI, *Optimal convergence of adaptive FEM for eigenvalue clusters in mixed form*, *Math. Comp.*, 86 (2017), pp. 2213–2237, <https://doi.org/10.1090/mcom/3212>.
- [14] D. BOFFI, L. GASTALDI, R. RODRÍGUEZ, AND I. ŠEBESTOVÁ, *Residual-based a posteriori error estimation for the Maxwell’s eigenvalue problem*, *IMA J. Numer. Anal.*, 37 (2017), pp. 1710–1732, <https://doi.org/10.1093/imanum/drw066>.
- [15] P. G. CIARLET, *The finite element method for elliptic problems*, North-Holland Publishing Co., Amsterdam-New York-Oxford, 1978. Studies in Mathematics and its Applications, Vol. 4.
- [16] R. G. DURÁN, L. GASTALDI, AND C. PADRA, *A posteriori error estimators for mixed approximations of eigenvalue problems*, *Math. Models Methods Appl. Sci.*, 9 (1999), pp. 1165–1178, <https://doi.org/10.1142/S021820259900052X>.
- [17] E. B. FABES, C. E. KENIG, AND G. C. VERCHOTA, *The Dirichlet problem for the Stokes system on Lipschitz domains*, *Duke Math. J.*, 57 (1988), pp. 769–793, <https://doi.org/10.1215/S0012-7094-88-05734-1>.
- [18] G. N. GATICA, L. F. GATICA, AND A. MÁRQUEZ, *Augmented mixed finite element methods for a vorticity-based velocity–pressure–stress formulation of the Stokes problem in 2D*, *Internat. J. Numer. Methods Fluids*, 67 (2011), pp. 450–477, <https://doi.org/10.1002/flid.2362>.
- [19] G. N. GATICA, L. F. GATICA, AND F. A. SEQUEIRA, *A priori and a posteriori error analyses of a pseudostress-based mixed formulation for linear elasticity*, *Comput. Math. Appl.*, 71 (2016), pp. 585–614, <https://doi.org/10.1016/j.camwa.2015.12.009>.
- [20] G. N. GATICA, A. MÁRQUEZ, AND M. A. SÁNCHEZ, *Analysis of a velocity–pressure–pseudostress formulation for the stationary Stokes equations*, *Comput. Methods Appl. Mech. Engrg.*,

- 199 (2010), pp. 1064–1079, <https://doi.org/10.1016/j.cma.2009.11.024>.
- [21] J. GEDICKE AND A. KHAN, *Arnold-Winther mixed finite elements for Stokes eigenvalue problems*, SIAM J. Sci. Comput., 40 (2018), pp. A3449–A3469, <https://doi.org/10.1137/17M1162032>.
- [22] J. GEDICKE AND A. KHAN, *Divergence-conforming discontinuous Galerkin finite elements for Stokes eigenvalue problems*, Numer. Math., 144 (2020), pp. 585–614, <https://doi.org/10.1007/s00211-019-01095-x>.
- [23] P. HUANG AND Q. ZHANG, *A posteriori error estimates for the Stoke eigenvalue problem based on a recovery type estimator*, Bull. Math. Soc. Sci. Math. Roumanie (N.S.), 62(110) (2019), pp. 295–304.
- [24] S. JIA, H. CHEN, AND H. XIE, *A posteriori error estimator for eigenvalue problems by mixed finite element method*, Sci. China Math., 56 (2013), pp. 887–900, <https://doi.org/10.1007/s11425-013-4614-0>.
- [25] T. KATO, *Perturbation theory for linear operators*, Die Grundlehren der mathematischen Wissenschaften, Band 132, Springer-Verlag New York, Inc., New York, 1966.
- [26] F. LEPE AND D. MORA, *Symmetric and nonsymmetric discontinuous Galerkin methods for a pseudostress formulation of the Stokes spectral problem*, SIAM J. Sci. Comput., 42 (2020), pp. A698–A722, <https://doi.org/10.1137/19M1259535>.
- [27] F. LEPE AND G. RIVERA, *A virtual element approximation for the pseudostress formulation of the stokes eigenvalue problem*, Computer Methods in Applied Mechanics and Engineering, 379 (2021), <https://doi.org/10.1016/j.cma.2021.113753>.
- [28] F. LEPE, G. RIVERA, AND J. VELLOJIN, *Mixed methods for the velocity-pressure-pseudostress formulation of the Stokes eigenvalue problem*, SIAM J. Sci. Comput., Accepted for publication (2022).
- [29] H. LIU, W. GONG, S. WANG, AND N. YAN, *Superconvergence and a posteriori error estimates for the Stokes eigenvalue problems*, BIT, 53 (2013), pp. 665–687, <https://doi.org/10.1007/s10543-013-0422-8>.
- [30] X. LIU, M. T. NAKAO, C. YOU, AND S. OISHI, *Explicit a posteriori and a priori error estimation for the finite element solution of Stokes equations*, Jpn. J. Ind. Appl. Math., 38 (2021), pp. 545–559, <https://doi.org/10.1007/s13160-020-00449-5>.
- [31] A. LOGG, K.-A. MARDAL, AND G. WELLS, *Automated solution of differential equations by the finite element method: The FEniCS book*, vol. 84, Springer Science & Business Media, 2012, <https://doi.org/https://doi.org/10.1007/978-3-642-23099-8>.
- [32] C. LOVADINA, M. LLYLY, AND R. STENBERG, *A posteriori estimates for the Stokes eigenvalue problem*, Numer. Methods Partial Differential Equations, 25 (2009), pp. 244–257, <https://doi.org/10.1002/num.20342>.
- [33] S. MEDDAHI, D. MORA, AND R. RODRÍGUEZ, *A finite element analysis of a pseudostress formulation for the Stokes eigenvalue problem*, IMA J. Numer. Anal., 35 (2015), pp. 749–766, <https://doi.org/10.1093/imanum/dru006>.
- [34] P. MONK, *Finite element methods for Maxwell's equations*, Oxford University Press, 2003.
- [35] J.-C. NÉDÉLEC, *Mixed finite elements in  $\mathbf{R}^3$* , Numer. Math., 35 (1980), pp. 315–341, <https://doi.org/10.1007/BF01396415>.
- [36] J.-C. NÉDÉLEC, *A new family of mixed finite elements in  $\mathbf{R}^3$* , Numer. Math., 50 (1986), pp. 57–81, <https://doi.org/10.1007/BF01389668>.
- [37] R. OYARZÚA, M. SOLANO, AND P. ZÚÑIGA, *A priori and a posteriori error analyses of a high order unfitted mixed-FEM for Stokes flow*, Comput. Methods Appl. Mech. Engrg., 360 (2020), pp. 112780, 40, <https://doi.org/10.1016/j.cma.2019.112780>.
- [38] G. SAVARÉ, *Regularity results for elliptic equations in Lipschitz domains*, J. Funct. Anal., 152 (1998), pp. 176–201, <https://doi.org/10.1006/jfan.1997.3158>.
- [39] L. SUN AND Y. YANG, *The a posteriori error estimates and adaptive computation of nonconforming mixed finite elements for the Stokes eigenvalue problem*, Appl. Math. Comput., 421 (2022), p. Paper No. 126951, <https://doi.org/10.1016/j.amc.2022.126951>.
- [40] R. VERFÜRTH, *A posteriori error estimation and adaptive mesh-refinement techniques*, in Proceedings of the Fifth International Congress on Computational and Applied Mathematics (Leuven, 1992), vol. 50, 1994, pp. 67–83, [https://doi.org/10.1016/0377-0427\(94\)90290-9](https://doi.org/10.1016/0377-0427(94)90290-9).
- [41] R. VERFÜRTH, *A posteriori error estimation techniques for finite element methods*, Numerical Mathematics and Scientific Computation, Oxford University Press, Oxford, 2013, <https://doi.org/10.1093/acprof:oso/9780199679423.001.0001>.